THE DETERMINATION OF THE COEFFICIENT OF THERMAL EXPANSION AND YOUNG'S MODULUS OF ELASTICITY OF HIGH LEAD GLASS

A THESIS

Presented to

The Faculty of the Graduate Division

by

Alan Robert Koenig

In Partial Fulfillment

of the Requirements for the Degree

Master of Science in Ceramic Engineering

Georgia Institute of Technology

June, 1965

THE DETERMINATION OF THE COEFFICIENT OF THERMAL EXPANSION AND YOUNG'S MODULUS OF ELASTICITY OF HIGH LEAD GLASS

Approved:

Chairman

Date approved by Chairman 5/31/65

In presenting the dissertation as a partial fulfillment of the requirements for an advanced degree from the Georgia Institute of Technology, I agree that the Library of the Institute shall make it available for inspection and circulation in accordance with its regulations governing materials of this type. I agree that permission to copy from, or to publish from, this dissertation may be granted by the professor under whose direction it was written, or, in his absence, by the Dean of the Graduate Division when such copying or publication is solely for scholarly purposes and does not involve potential financial gain. It is understood that any copying from, or publication of, this dissertation which involves potential financial gain will not be allowed without written permission.

3/17/65
b

ACKNOWLEDGMENTS

I am deeply indebted to Dr. W. E. Moody, Jr. for his interest and help, not only concerning this work, but at every stage of my graduate studies. My appreciation is also expressed to Dr. W. W. Hines for his willing assistance with many problems, and to Dr. L. Mitchell and Dr. H. M. Wadsworth for their interest and their suggestions while serving on the reading committee.

The International Lead-Zinc Research Organization, through fellowship program LC-51, made it possible for me to devote full time to academic work, and my deepest appreciation is due for this assistance. I wish to thank Mr. W. S. Fleming, of the Rich Electronic Computer Center, for his assistance with the computer programming. Thanks are also extended to Mr. T. Mackrovitch for his help with the machining work. A large portion of the raw materials for this work were generously furnished by the Titanium Alloy Division of the National Lead Company.

The encouragement and assistance of my wife, Sharon, my parents, Mr. and Mrs. M. G. Koenig, and many other relatives, particularly Mr. and Mrs. A. Skott, are gratefully acknowledged. The excellent typing of the draft by Mrs. M. Watson is deeply appreciated.

TABLE OF CONTENTS

Page

ACKNOWLEDGMENTS ii

LIST OF TABLES v

LIST OF ILLUSTRATIONS viii

SUMMARY ix

CHAPTER

I. INTRODUCTION 1

II. SURVEY OF LITERATURE 3

III. INSTRUMENTATION AND EQUIPMENT 17

Glass Smelting
Fiber Drawing Apparatus
Thermal Expansion Measurement Equipment
Young's Modulus Measurement Equipment

IV. PROCEDURE 29

Composition Selection
Specimen Preparation
Coefficient of Thermal Expansion
Young's Modulus

V. DISCUSSION OF RESULTS 37

Raw Material Selection
Sample Preparation
Coefficient of Thermal Expansion
Design One
Design Two
Young's Modulus
Design Three
Design Four

VI. CONCLUSIONS 64

TABLE OF CONTENTS (Continued)

APPENDICES Page

A. BATCH COMPOSITIONS 69

B. LINEAR REGRESSION 74

C. ANALYSIS OF DESIGN ONE 78

D. MULTIPLE REGRESSION ANALYSIS PROGRAM 86

E. ANALYSIS OF DESIGN TWO 88

F. ANALYSIS OF DESIGN THREE 103

G. ANALYSIS OF DESIGN FOUR 107

BIBLIOGRAPHY 121

LIST OF TABLES

Table		Page
1.	Factors for Calculation of Linear Coefficient of Thermal Expansion in in./in./°C	10
2.	One-Third Replicate of 3^5 Design	31
3.	Coefficient of Thermal Expansion x 10^6 in./in./°C. Design One	45
4.	Analysis of Variance Design One	46
5.	Coefficient of Thermal Expansion Equations Design One	47
6.	Coefficient of Thermal Expansion x 10^6 in./in./°C	49
7.	ANOVA Coefficient of Thermal Expansion Design Two	50
8.	Coefficient of Thermal Expansion Equations Design Two	52
9.	Young's Modulus in Kilobars Design Three	56
10.	Young's Modulus ANOVA Design Three	57
11.	Young's Modulus Equations Design Three	59
12.	Young's Modulus in Kilobars Design Four	60
13.	ANOVA Young's Modulus of Elasticity Design Four	61
14.	Equations for Young's Modulus Design Four	63
15.	Batch Compositions	69
16.	Expansion Data Composition 70	75
17.	Calculation of the Regression Equation	77
18.	Analysis of Variance Worksheet	78
19.	Analysis of Variance Design One	81
20.	Duncan's Multiple Range Test	84
21.	Standard Deviation Due to Experimental Error	85

LIST OF TABLES (Continued)

Table		Page
22.	Data Summed Over Factors CDE	90
23.	Data Summed Over Factors BDE	91
24.	Data Summed Over Factors BCE	92
25.	Data Summed Over Factors BCD	93
26.	Data Summed Over Factors ADE	94
27.	Data Summed Over Factors ACE	95
28.	Data Summed Over Factors ACD	96
29.	Data Summed Over Factors ABE	97
30.	Data Summed Over Factors ABD	98
31.	Data Summed Over Factors ABC	99
32.	Duncan's Multiple Range Test for Interactions Design Two	101
33.	Best Estimate of the Magnitude of the Residual Interactions Plus Experimental Error Design Two	102
34.	Duncan's Multiple Range Test Design Three	105
35.	Standard Deviation Due to Experimental Error in Kilobars Design Three	106
36.	Data Summed Over Factors CDE	108
37.	Data Summed Over Factors BDE	109
38.	Data Summed Over Factors BCE	110
39.	Data Summed Over Factors BCD	111
40.	Data Summed Over Factors ADE	112
41.	Data Summed Over Factors ACE	113
42.	Data Summed Over Factors ACD	114
43.	Data Summed Over Factors ABE	115

LIST OF TABLES (Continued)

Table		Page
44.	Data Summed Over Factors ABD	116
45.	Data Summed Over Factors ABC	117
46.	Duncan's Multiple Range Test for Interactions Design Four	119
47.	Best Estimate of the Magnitude of the Residual Interactions Plus Experimental Error	120

LIST OF ILLUSTRATIONS

Figure		Page
1.	Section View of Induction Crucible Furnace	19
2.	Fiber Drawing and Glass Smelting Apparatus	21
3.	Gaertner Quartz-Tube Dilatometer	23
4.	Section View of Phonograph Pickup	26
5.	Lissajous Ellipses	26
6.	Young's Modulus Measurement Equipment	28
7.	Thermal Expansion Composition 70	76
8.	Average Values of Coefficient of Expansion x 10^6 in./in./°C.	82
9.	Average Values of Coefficient of Expansion x 10^6 in./in./°C.	100
10.	Average Values of Coefficient of Expansion x 10^6 in./in./°C.	100
11.	Average Values of Young's Modulus in Kilobars	104
12.	Average Values of Young's Modulus in Kilobars	118
13.	Average Values of Young's Modulus in Kilobars	118

SUMMARY

Recently there have been developed numerous processes for the manufacture of lightweight ceramic aggregate block, which possesses an extremely low coefficient of thermal expansion. Therefore, glazes covering these blocks must also have a low coefficient of thermal expansion or high elasticity, or both.

The purpose of this research was to investigate Young's modulus and the coefficient of thermal expansion of glasses in the composition ranges generally employed in fast-fire glazing. Since it would be impossible to examine all possible glaze components in one project, this work covers only the common variation in the R_2O_3 and RO_2 groups. The regions of glaze composition studied were:

1	PbO	0 - 0.375 B_2O_3	1.0 - 2.0 SiO_2
		0 - 0.200 Al_2O_3	0 - 0.200 TiO_2
			0 - 0.200 ZrO_2

The glass compositions used for determining the properties of interest were chosen by use of factorial designs. Two designs were employed for each of the properties to be investigated, Young's modulus and the linear coefficient of thermal expansion. Thermal expansion measurements were made by use of the quartz tube dilatometer method. The temperature vs. cumulative expansion data was analyzed by the method of Linear Regression to obtain the coefficient. Young's modulus measurements were made by use of a sonic technique to determine the

velocity of sound through a fiber drawn from a melt of the desired composition. Values of the modulus were found by multiplying the square of the velocity of sound through the fiber by the density of the glass.

In the composition regions investigated, coefficient of thermal expansion for many of the glasses were somewhat lower than predicted using classical data. Zirconia, alumina, and silica reduce coefficient of expansion, while titania and boron have little effect. In the region of composition:

1 PbO 0 - 0.375 B_2O_3 1.0 - 2.0 SiO_2

the multiple regression equation that fit the collected data most satisfactorily was:

$$\alpha = 13.48 \times 10^{-6} - 2.10 \times 10^{-6} X_1 - 2.92 \times 10^{-6} X_2 + 6.36 \times 10^{-7} X_1X_2$$

where: X_1 = equiv. B_2O_3 X_2 = equiv. SiO_2

α = coefficient of thermal expansion in in./in./°C.

In the region of composition:

1 PbO 0 - 0.250 B_2O_3 1.0 - 2.0 SiO_2

0 - 0.200 Al_2O_3 0 - 0.200 TiO_2

0 - 0.200 ZrO_2

the equation that fit the collected data best was:

$$\alpha = 11.89 \times 10^{-6} + 0.55 \times 10^{-6} X_1 - 1.80 \times 10^{-6} X_2 - 4.75 \times 10^{-6} X_3 + 0.24 \times 10^{-6} X_4 - 7.77 \times 10^{-6} X_5 - 0.03 \times 10^{-6} / X_2 X_3$$

where: X_1 = equiv. B_2O_3 X_2 = equiv. SiO_2

X_3 = equiv. Al_2O_3 X_4 = equiv. TiO_2

X_5 = equiv. ZrO_2

α = coefficient of thermal expansion in in./in./°C.

Young's moduli for all the glass compositions studied were somewhat lower than most other glasses used in glazing work. This fact accounts for the low scratch resistance of high lead glasses, and also accounts for their being somewhat more elastic due to being less brittle. In the region of composition:

1 PbO 0 - 0.375 B_2O_3 1.0 - 2.0 SiO_2

the best regression equation developed for Young's modulus was:

$$E = 186 + 224 X_1 + 346 X_2 - 106 X_2^2$$

where: X_1 = equiv. B_2O_3 X_2 = equiv. SiO_2

E = Young's modulus in Kilobars

In the region of composition:

1 PbO 0 - 0.350 B_2O_3 1.0 - 2.0 SiO_2

0 - 0.200 Al_2O_3 0 - 0.200 TiO_2

0 - 0.200 ZrO_2

the regression equation that fits the data most accurately was:

$$E = 4.68 + 236\ X_1 + 182\ X_2 + 308\ X_3 + 101\ X_4 + 126\ X_5 + 94\ X_3X_5$$

where: X_1 = equiv. B_2O_3 X_2 = equiv. SiO_2

X_3 = equiv. Al_2O_3 X_4 = equiv. TiO_2

X_5 = equiv. ZrO_2

E = Young's modulus in Kilobars

CHAPTER I

INTRODUCTION

In recent years numerous processes for the manufacture of low-thermal-expansion lightweight ceramic aggregates have been developed. Shapes made of these aggregates are particularly adaptable to fast-fire glazing due to their low coefficient of thermal expansion. Linear coefficient of expansion of some lightweight aggregate blocks is as low as 2.5×10^{-6} in./in./°C. According to classical data, commercial type glazes with low melting constituents are virtually impossible to develop with a coefficient of expansion lower than 7.0×10^{-6} in./in./°C. If a glaze with an expansion this great is applied over a composition of low expansion, crazing should result. Yet glazes have been developed which do not craze when applied over these compositions.

There seem to be three logical answers to this non-crazing phenomenon. First, available data is not applicable in the regions of composition used for fast-fire glazing. Second, if glazes possess an exceptionally low Young's modulus, a fairly large difference in expansion between body and glaze might be tolerated. Finally, some combination of the first two answers may be responsible.

The purpose of this research was to investigate Young's modulus and the coefficient of thermal expansion in the composition ranges generally employed in fast-fire glazing. To investigate all the possible ingredients in fast-fire glazes would be well beyond the scope of this

investigation. Therefore, this work covers only common variations in the R_2O_3 and RO_2 groups for glazes. The RO group was held constant at one equivalent of lead oxide.

The concepts of statistical experimental design have been used in setting up the mode of attack on the problem. Results have been tabulated and interpreted with the help of various statistical techniques. Finally, the collected data were used to develop equations for the calculation of Young's modulus and the coefficient of thermal expansion within the range of compositions studied.

CHAPTER II

LITERATURE SURVEY

Recently numerous processes for the manufacture of lightweight ceramic aggregates have been developed. These products are lightweight due to bloating of the raw clay, shale, volcanic ash, or slag used. This is usually accomplished in a rotary furnace into which the aggregate former is introduced. Bloating is caused by the violent evolution of gases contained in the clay or materials added to the clay which produce gas. One of the most common gas-producing reactions is the reduction of iron oxide to the ferrous state. Other important gas formers are the carbonates, sulfates, and organic additions sometimes added to the bloating mix such as wheat flour and starches. Bloating is caused by the large amounts of gas evolved during heating.

Generally speaking, all ceramic aggregates have one thing in common. They are lightweight because of the large amount of open space contained in their structure. This property of lightness in weight makes these substances ideal for structural clay products, especially bricks, building blocks, and curtain walls. Not only would these materials lighten building loads on other components, but also would permit larger pieces to be handled.

Structural clay products manufacturers have realized these advantages, and many of them are now experimenting with the production of lightweight ceramic building materials. Aggregates, in general, cannot be formed into various shapes without the addition of some sort of binder.

The most common bonding material is clay. Good results are obtained using a composition of about 50 per cent clay plus 50 per cent aggregate by volume. Compacting methods generally used are dry pressing and vibratory compaction. Recently some experiments have been performed on extruding clay bonded lightweight block with only fair success due to the abrasive nature of the grain. The difficulty in using such a high percentage of clay is that a large portion of the lightness is lost. Several other bonding methods are being tried, among which is a process using relatively small amounts of bentonite. Other partially successful binders have been sodium silicate, rasorite (sodium borate), and lead monosilicate.

When a bonded lightweight aggregate block is heated it shows a remarkably low coefficient of thermal expansion. This is apparently due to the fact that the individual grains, having a large proportion of internal open space to solid material, have room to expand themselves and into other grains without materially increasing the length of the whole body during heating. Consequently, lightweight aggregate bodies have good thermal shock resistance.

Manufacturers, noting that a glazed block would bring a high premium, have been anxious to find glazes to apply over these compositions. Also, due to the good thermal shock resistance of the bodies, it has been felt that these materials would present an ideal application for a fast-fire glazing process. In the past few years a great deal of research time has been expended in this pursuit by glaze manufacturers.

The desirable properties of glazes for structural clay products are numerous. The glaze should be craze free, to prevent moisture from entering the block, and also, for appearance sake. It should withstand

repeated freezing and thawings. It should be resistant to scratching, and tough enough to resist punctures. Acid resistance should be high enough to withstand many years of exposure to the atmosphere. Detergent resistance should be good enough to withstand repeated cleanings. The glaze should add to the beauty of the product it is covering. The color should be uniform and the degree of gloss, whether matte or high gloss, should be consistent.

Generally speaking, fast-fire glazes should mature at a low temperature. The low temperature condition is important, because the lower the temperature the faster the body and glaze can be brought up to this temperature. It is well known that body and glaze need not exactly match in coefficient of expansion for the production of a craze free product. This is due to the fact that an interfacial layer is built up between the glaze and the body during conventional slow firing, and the mismatch in expansion between adjacent microscopic layers is not nearly as great as if the absolute difference between body and glaze were considered. In fast-firing, however, there is no time for interfacial layers to develop.

Furthermore, in order to obtain a satisfactory fit between a glaze and a body, it is desirable to have the glaze be in a condition of compression. This is necessary, in that crazing is caused by tensil stresses developed in the glaze. However, if the glaze is put under too high a compressive stress, a defect known as "shivering" or failure under compressive stresses takes place. Even when compressive stress has been developed, delayed crazing failures may occur. Silicate bodies tend to increase in volume because of moisture expansion. Expansion of the body decreases the

compression of the glaze and transforms the stress into tension, and after sufficient time the ware tends to craze. Thus, in order to prevent crazing, it is desirable to have substantial initial compressive stress.

The term "fast-firing" may be defined as a process whereby a ceramic product with applied glaze is matured at temperatures generally between 800°C. and 1050°C., in a cycle ranging from one hour to four hours. Fast-fire coatings are not new, as there are available years of experience involving glass enamels which are fired through lehrs in cycles ranging from 15 minutes to 1-1/2 hours, and porcelain enamels which are fired through furnaces in cycles ranging from 5 to 15 minutes. However, fast-fire glazes covering low coefficient of thermal expansion bodies is an area in which relatively little work has been done until recently.

During conventional firing of glazes there is a long period of time for the glaze to adjust itself to the various conditions that present themselves. In fast-firing this time element is lacking, and the applied glaze has to have various special features built into it. It is in this field that fast-firing has borrowed heavily from glass enamels and porcelain enamels.

During rapid-firing the components of the glaze do not have time to migrate and react with one another. Also, any gases given off by the raw materials during firing, such as water vapor and carbon dioxide, would cause holes or bubbles in the glaze surface which would not have time to heal during the short firing period. For these reasons, it is deemed necessary to frit fast-fire glaze compositions. The faster the firing schedule,

the higher the percentage of frit required. In fact, for very rapid fire glazes, five minutes to one hour, it is deemed necessary to have nearly 100 per cent frit. This means that only extremely small amounts of clay can be added to the frit.

With slow firing cycles it is possible to cover up many faults in poor glaze application. Most glazes achieve a certain degree of fluidity during the firing cycle, and tend to level themselves, producing a smooth coat. As the firing cycle is decreased the available time to complete this process is reduced. It turns out that the glaze surface retains all spraying defects. For this reason special attention must be given to the spray medium of the glaze.

Many special organics must be added to the glaze to improve sprayability. Also, due to lack of clay in the glaze suspension, different suspending mediums must be found for the frits which are unusually heavy due to the large amounts of lead oxide usually contained. Finally, special organic additions must be found to enhance the green strength of the glazes due to the lack of clay which usually performs this function.

As was stated earlier, the coefficient of expansion of lightweight aggregate bodies is quite low. On some of these bodies the linear expansion is as low as 2.5×10^{-6} in./in./°C. When a glaze is applied over a body the coefficients of expansion of the adjoining layers must be equal, or stresses will be developed. Under these conditions the stresses are the same as if the sample were allowed to expand freely and then compressed back to its original size by an applied restraining force. The stress required is proportional to the elasticity of the material and the elastic strain, which is equal to the product of the thermal expansion and temperature

change. For a perfectly elastic rod restrained in only one direction,

$$\sigma = Ea(T' - T_o) \qquad (1)$$

where σ is the stress in psi, E is the modulus of elasticity, a the linear expansion coefficient, T_o the initial temperature, and T' the new temperature level.

On heating, stresses resulting from restraints are compressive, since the body tends to expand against the restraining member. On cooling, similar tensile stresses can result. Tensile stresses are developed in a glaze by firing on an underlying body of smaller thermal expansion coefficient than the glaze, and tensile stresses in a glaze are the cause of crazing.

The expansion coefficient of a glaze depends mainly on the network structure. Since the individual atoms in the structure are held by a balance of attractive and repulsive forces, the addition of thermal energy to the structure upsets the balance, and an increase in length is noted. This increase in length may be expressed as the coefficient of linear expansion, or expansivity which is defined as the ratio of the change in length per degree C. to the length at zero degrees C. If desired, this figure can be expressed as the coefficient of volume expansion, which is to a first approximation equal to three times the linear coefficient of expansion. Both types of expressions are used in the literature, and great care must be used in specifying which one is referred to. The units generally used for expressing the linear expansion are in./in./°C.

According to Morey (42) the coefficient of expansion is roughly an additive property of a glass. Over the range in which the expansion is

approximately a linear function of temperature, the coefficient of expansion of a complete glaze may be calculated on the assumption of additivity by means of the equation.

$$\alpha = a_1p_1 + a_2p_2 + \ldots + a_np_n \qquad (2)$$

in which α is the linear coefficient of expansion, $p_1, p_2, \ldots, p_n$ are the percentages by weight of the various components, and $a_1, a_2, \ldots, a_n$ are the constants for various oxides commonly employed in glazes. In Table 1 are assembled the factors for the calculation of the coefficient of expansion proposed by several authors. The work of Winkelman and Schott (61) is classic in this field. The factors proposed by English and Turner (23) are considered among the most reliable. They are based largely on trisilicate glasses. Gilard and Dubrul (27) discussed the calculation of the coefficient of expansion from the composition, and proposed a set of factors of the type

$$a \times 10^8 = (ax + bx^2) \qquad (3)$$

in which x represents the percentage by weight of a given constituent, and a and b are empirical factors. The tables presented by Bryant (10) are of help in obtaining factors for expansion not listed elsewhere.

The other important factor in determining the craze resistance of a glaze is the modulus of elasticity. The property by which a glass regains its original dimensions, after being strained by the action of an applied force, is called elasticity. A substance is said to be elastic when on being left free, it recovers wholly or partially from a deformation. Glass is an elastic substance at ordinary temperatures, according to this

Table 1. Factors for Calculation of Linear Coefficient of Thermal Expansion in in./in./°C.*

Material	Winkelmann and Shott	English and Turner	Bryant
SiO_2	2.67	0.50	2.67
B_2O_3	0.33	-6.53	
Na_2O	33.33	41.63	
K_2O	28.33	39.00	
MgO	0.33	4.50	
CaO	16.67	16.30	
ZnO	6.00	7.00	7.00
BaO	10.00	14.00	
PbO	10.00	10.60	
Al_2O_3	16.67	1.40	16.67
ZrO_2			7.00
TiO_2			13.33

definition, if the applied force is not held for too long a period. This elastic extension of a material corresponds to uniformly increasing the separation between the atoms of the structure. As a result, elastic extension is related directly to the forces between atoms and the structure energy. Many more or less satisfactory correlations between lattice energy and elastic modulii have been proposed and work quite well for

*Factors shown have been multiplied by 10^8.

materials with the same structure and bond type. Generally speaking, crystals with low thermal expansion have a high modulus of elasticity.

Hooke's law states that stress is proportional to a strain. Throughout the region in which Hooke's law applies, the material is perfectly elastic by definition, and the limit beyond which the strain is no longer proportional to the deforming stress is called the elastic limit. The breaking point of glass has been found at the elastic limit. The constant of proportionality for each type of stress is a characteristic property. The behavior under stress is described by the elastic moduli, each of which represents the ratio of a stress to a strain. The specification of the strains resulting from a system of stresses applied to an elastic substance requires in the most general case the specification of 21 elastic constants. However, if the material is isotropic the number of constants is reduced to two. Commonly used modulii are the modulus of rigidity, or bulk modulus, K; and the modulus of extension in tension, or Young's modulus, E. Young's modulus can be expressed in terms of the other above named moduli by the equation:

$$E = \frac{9KR}{3K + R} \qquad (4)$$

The unit generally used to express Young's modulus of glasses is the kilobar, which is equal to 10^9 dyne cm^2.

The classic work on the determination of the elastic constants of glasses was done by Winkelmann and Schott (61). The results of their experiments are the chief source of information as to the magnitude of Young's modulus for many types of glass. Their work is supplemented by

the work of Staubel (55), who determined the value of Poisson's ratio for a number of the same glasses. Clark and Turner (14) studied the effect of systematic changes in composition on the properties of a series of glasses. However, on the whole only a relatively small amount of reliable work has been done on the elastic constants of glass, and almost none on the compositions for low temperature glaze work.

Since the linear coefficient of expansion of a typical lightweight aggregate block is around 2.5×10^{-6} in./in./°C., a glaze having a linear coefficient of expansion as low or lower than this is needed if compression of the glaze is to be maintained and crazing avoided. However, it is well known that the glaze does not have to actually have as low a coefficient of expansion as the body to remain craze free. The difference in expansion between glaze and body is commonly known as mismatch. It is generally accepted that the mismatch can be as large as 1.0×10^{-6} or even slightly larger. This is most probably due to the fact that glazes can stand a small amount of tensile stress, and also that glazes are somewhat elastic and have some give.

When any combination of glaze materials is used to make a low temperature glaze for a lightweight aggregate body, it can be seen from the data in Table 1 that it will produce a glaze having a linear coefficient of expansion in the neighborhood of 7.0×10^{-6}. This is clearly above the region where the glaze should fit the body. Recent experiments have shown that a craze-free glaze can be made for lightweight aggregate blocks incorporating most all the attributes of a good structural clay products glaze. The question that has not been answered is, how is this possible in the light of current glaze theory? It seems that this question

has many possible answers.

First, existing coefficient of expansion data is not entirely applicable for the compositions used for fast-fire glazes. The existing data was obtained for glasses of quite different proportions than those used in fast-fire glazing. It is also known that existing data is not exact, and many deviations from the listed values occur. Also, the published data does not entirely agree even among itself, as seen in Table 1. Thus, in the compositions of interest in fast-fire glazing, the linear coefficient of expansion of the glaze may be lower than expected.

Second, it would seem reasonable to expect that glazes having a lower modulus of elasticity could withstand a greater mismatch in expansion between glaze and body without crazing. Existing data on this phase of the problem is very sparse, and furthermore, there is no data in the particular regions of interest to fast-fire glazing. This is tied in with the other possible answer to the paradox, in that possibly a greater mismatch between body and glaze can be tolerated than is usually thought possible.

Fast-fire glazes generally start with a lead boro-silicate as the basic glass. Silica is the primary glass former. In general, an increase of silica in a glass will raise melting temperature, decrease fluidity of the melt, increase the resistance of the matured glaze to solution by water and to chemical attack, lower the coefficient of expansion, and increase the hardness and strength. Boron is used in fast-fire glazes because it is easily fusible and miscible in most silicate fusions, it lowers the coefficient of expansion of some glasses to a certain extent, is a moderately active flux, does not crystallize from fusions, and also tends to hinder the crystallization process of other compounds, thereby

preventing devitrification. Boron lowers the chemical durability of a glaze very rapidly as it is increased. Lead oxide is the primary flux in fast-fire glazes. Lead, when added to a glaze, increases the brilliancy of the glaze, lowers the coefficient of expansion as compared to the alkaline fluxes, increases elasticity of a glaze, and decreases the viscosity of the melt. The use of lead compounds in glazes have some disadvantages, such as the poisonous nature of lead compounds, the lowering of acid resistance when used in large quantities, and the lowering of abrasion resistance.

In addition to lead, the RO group of fast-fire glazes may contain small amounts of lithium oxide, sodium oxide, potassium oxide, magnesium oxide, calcium oxide, strontium oxide, barium oxide, zinc oxide, sodium fluoride, and calcium fluoride. Generally, it has been found that the alkalies increase the expansion of the glaze materially. However, they are excellent fluxes, and in some cases small amounts of these materials can be tolerated. Of this group, lithium probably increases the expansion the least, and is therefore preferable, but it materially increases the cost of the frit. The alkaline earths are frequently used in fast-fire glazes, and each imparts its own specific properties. Calcium increases abrasion resistance and decreases thermal expansion, while increasing tensile strength. It is a poor flux in low temperature glazes. Strontium is generally considered a mild flux and generally increases the fluidity of the melt. It has a little higher coefficient of thermal expansion than the other alkaline earths. Magnesium lowers the coefficient of expansion of a melt to a much greater degree than any other base, but its use in a low temperature glaze is limited due to its refractory nature.

Barium is a more vigorous flux than the other alkaline earths. It has a moderate coefficient of expansion. Zinc oxide has the greatest effect of any of the usual basic glaze components excepting calcia and magnesia in increasing the elasticity of a glaze. It is second only to magnesia in its power to lower the coefficient of expansion of the melt. With the exception of calcia it ranks first in increasing the strength. The alkaline fluorides are good fluxes and sometimes their inclusion in a low temperature glaze is desirable, but they have a marked effect in reducing the durability of a glaze.

The R_2O_3 group of a fast-fire glaze may be found to contain borom and aluminum oxides. The effect of boron has already been discussed. Alumina increases the hardness and other mechanical properties of a glaze, also its resistance to chemical action, including weathering. It has also been found useful in correcting crazing in some glazes. Alumina additions to a glaze increase refractoriness and viscosity.

Finally, the RO_2 group may contain silica, titanium, and zirconium. The functions of silica is a fast-fire glaze have already been explained. Titania acts somewhat similarly to silicon in the physical properties it imparts, and it also has a tendency to produce opacity in glazes, as it is only slightly soluble in the melts. The coefficient of thermal expansion is midway in the list of common oxides. The major value of titania in a lead glaze is its ability to improve acid resistance of the glaze. Zirconia is now used as the prime opacifier in almost all glazes. There are indications that zirconium oxide and other zirconium compounds materially lower the coefficient of expansion of glazes. Zirconia is a refractory compound and increases the melting temperature of the glass. It is

only slightly soluble in the melt, crystalizzing out as zirconium silicate which produces the opacity in glazes. Zirconia is essential to the production of glazes having good alkali resistance.

CHAPTER III

INSTRUMENTATION AND EQUIPMENT

Glass Smelting

Glass smelting was done in a small crucible furnace. This furnace was quite simple in design, containing a graphite core susceptor with insulation around it. A fireclay crucible containing the powdered materials to be smelted was placed into the graphite susceptor. Actual smelting was done in the fireclay crucible. Heat was supplied to the melting crucible from the graphite, which was heated by induction heating through the use of an Ajax six kilowatt converter.

The six kilowatt converter is a frequency changer designed to convert 60 cycle line current to high frequency current of approximately 30,000 cycles. The frequency range delivered by the converter varies from about 20,000 to 40,000 cycles, depending on the size of the furnace connected to the converter, and the load in the furnace.

The converter consists essentially of a high voltage transformer, a mercury arc spark gap, capacitors and an induction coil. The spark gap contains an electrode, a pool of mercury, and a means of controlling the level of the mercury in a manner which will allow the mercury pool level to be adjusted from a position where the electrode touches the mercury to a position with a space of about 5/16 in. between the tip of the electrode and the mercury pool. The capacitors are charged by the high voltage transformer until they have sufficient charge to cause a breakdown or arc

to occur between the mercury pool and the electrode. When the breakdown occurs, a high frequency current flows through the inductor coil. The high frequency current flowing in the inductor coil is not a uniform sine wave current, but is a series of damped oscillations. These oscillations occur three to five times during each half cycle of the 60 cycle input voltage. The frequency of the oscillations depends upon the load conditions in the inductor coil. The inductor coil is fabricated from high-conductivity copper tubing which serves as a medium for the cooling water as well as the electrical conductor. The coil used in this case had a six in. inside diameter.

In the furnace used, heating was accomplished by the alternating magnetic field flux inducing circulating currents in the graphite susceptor, which acts as a big resistor. This heat is in turn transferred to the fire clay crucible by the heat transfer processes of conduction and radiation. The raw materials are heated and melted in the crucible. A section drawing of the furnace is shown in Figure 1.

Fiber Drawing Apparatus

A glass fiber drawing apparatus was constructed for this work. The fiber was drawn through platinum bushings and wound on a plexiglas drum. The melting of the glass was accomplished in a platinum crucible, 0.040 in. wall thickness, which had three bushings in the bottom. Bushing openings were 0.035, 0.045, and 0.100 in. in diameter respectively. The two largest holes were kept plugged except during draining of the crucible at the conclusion of a run. The crucible was contained in a bubbled alumina and fused silica refractory combination. Heat was generated in

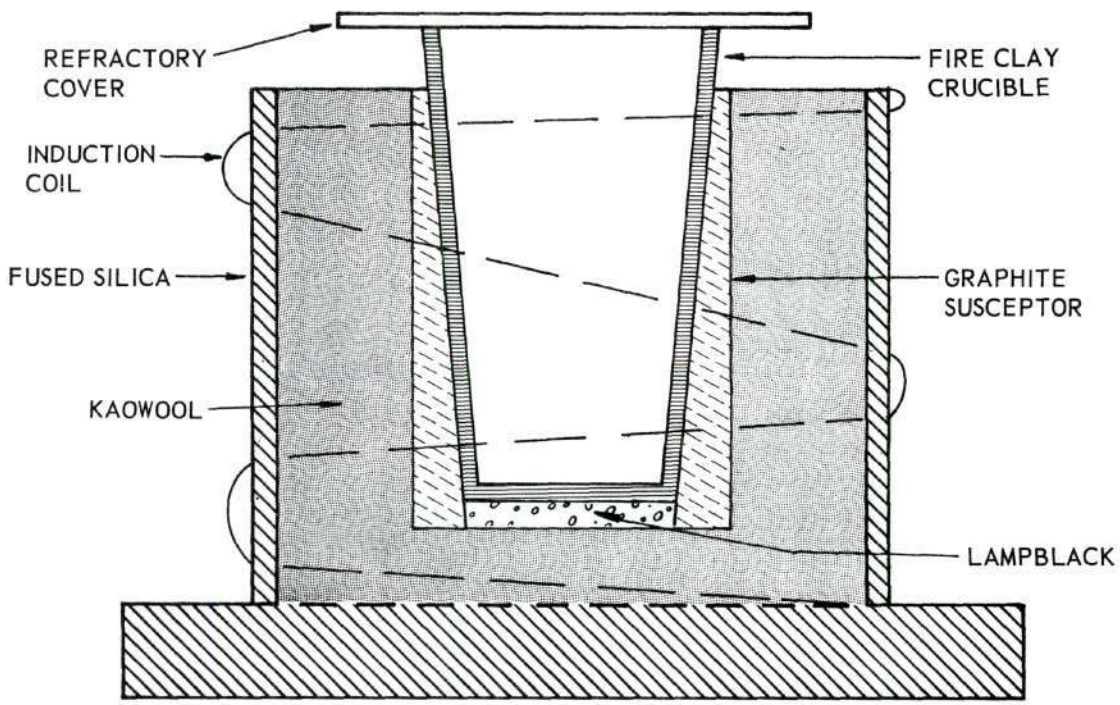

Figure 1. Section View of Induction Crucible Furnace.

the crucible by use of induction heating using the generator previously described. Temperature control was by a platinum-platinum rhodium thermocouple welded to the crucible. The couple was connected to a Wheelco program control. The signal from the control was used to operate an on-off contact installed in the induction generator. When the crucible reached the desired temperature, the contact was electrically broken and the generator turned off. When crucible temperature dropped 11°C., the contact closed electrically and the generator turned on again. Thus any desired temperature could be held ±11°C. As the glass reached the proper drawing temperature, a bead of molted glass formed on the outside of the bushing. This bead was pulled away from the crucible with a platinum wire, pulling a fiber along with it. The fiber was attached to a five in. diameter plexiglas drum with a piece of tape. The drum was eight in. long and had aluminum hubs on the end to prevent the fiber from slipping off the drum. It was rotated at a constant rate of between 30 and 140 rpm, depending on the glass composition by a speed controlled Dayton gearhead motor. A reciprocating mechanism was used to move a graphite thread guide along the drum, winding the fiber on the drum evenly. The mechanism was run by another Dayton gearhead motor and motor controller. The motor was attached to an eight in. diameter brass disk. As the disk revolved, it moved a brass rod back and forth in front of the plexiglas drum. Attached to this rod was a graphite thread guide. Figure 2 is a photograph of this equipment.

Thermal Expansion Measurement Equipment

There are several accepted methods of measuring the coefficient of

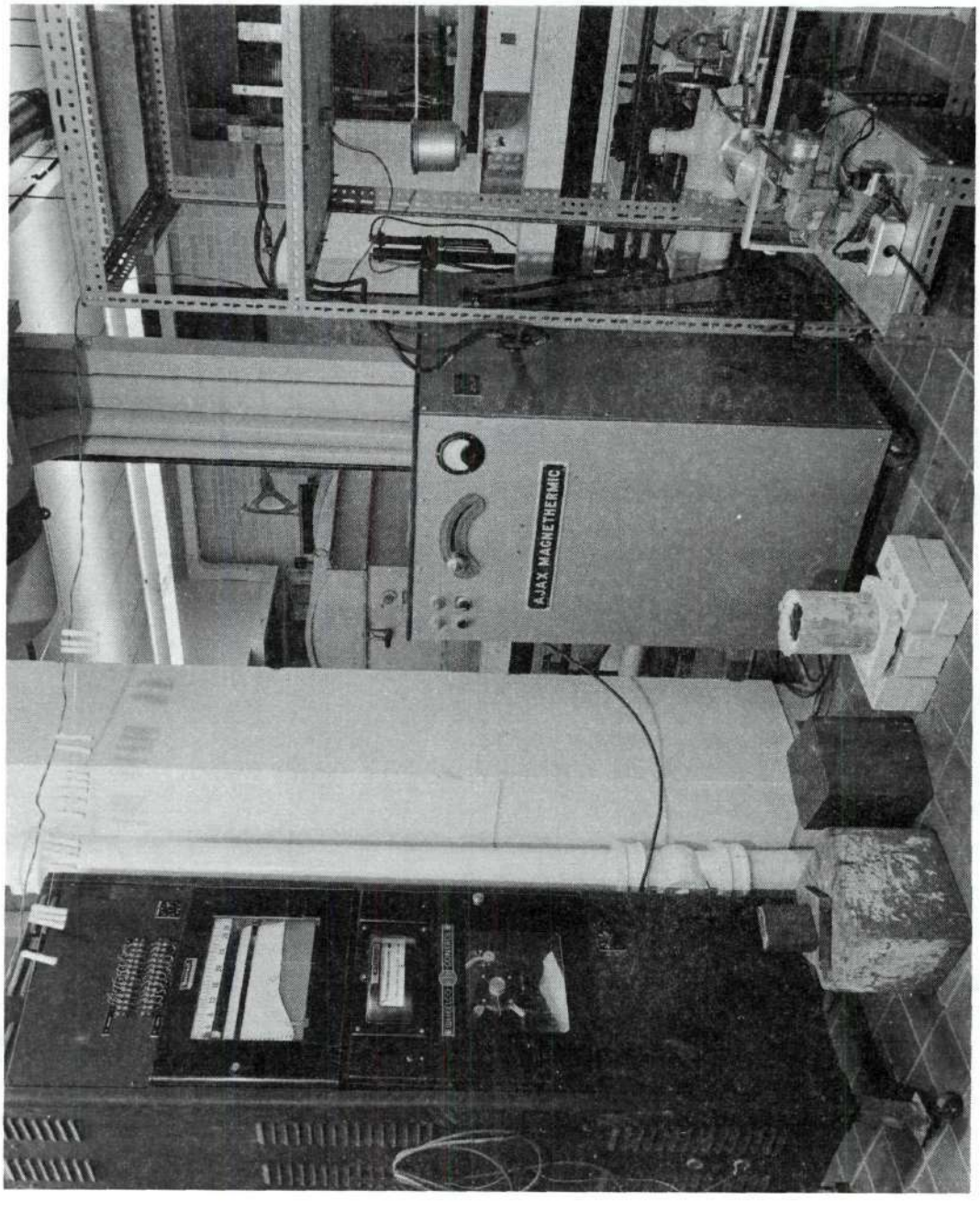

Figure 2. Fiber Drawing and Glass Smelting Apparatus.

thermal expansion. The most popular among these are the interferometer method, the quartz-tube dilatometer, and a method employing the degree of curvature of a thin double thread of glass commonly used in Europe. The method chosen for these experiments was the quartz-tube dilaletometric type, because of its ease of operation. The apparatus was of commercial origin and manufactured by Gaertner Scientific Corporation. A photograph of the apparatus is shown in Figure 3.

The Quartz-Tube Dilatometer is used to measure the linear coefficient of expansion of specimens up to 1/2 in. in diameter and from 2 to 3 in. long. It is designed to permit observations at temperatures up to 1000°C. The dilatometer holding the specimen and measuring its change consists of two tubes and a dial gage, thus eliminating the use of viewing apparatus as is required by the interferometer method. The two tubes are made of fused quartz, one fitting within the other. The outer tube is 14 in. long, has an inside diameter of 11/16 in., and is closed at its lower end. Near the lower end of the tube, a portion of its side, three in. long, is cut away to form a window through which the specimen is placed in position for test. The inner tube, both ends of which are closed, is three in. shorter than the outer tube and 5/8 in. outside diameter, so as to fit snugly without binding inside the outer tube. The dial gage indicator is a commercial type of high precision gage, calibrated to read 0.0001 in. per division. It is securely mounted at the upper end of an invar bracket with the stem of the gage extending downward and being aligned with the tube axis. An adjustment is provided for vertical positioning of the dial gage to permit various sample lengths.

The furnace, rated at 1250 watts, is a commercial tube type fitted

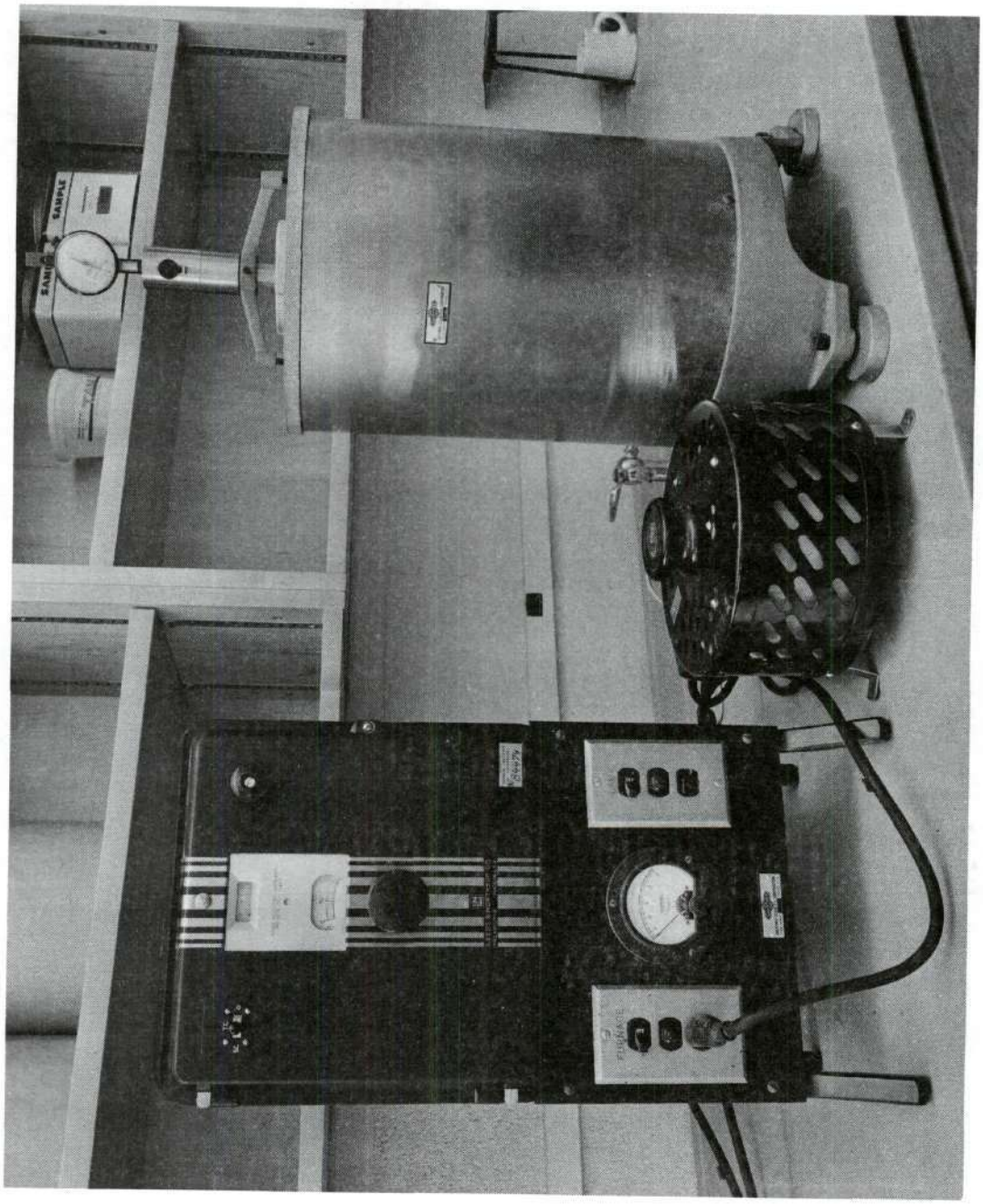

Figure 3. Gaertner Quartz-Tube Dilatometer.

with special brackets to support the dialatometer in the center. It is sealed off at the bottom by a refractory plate which supports a thermocouple that fits directly under the center of the quartz tube. The couple is of the chromel-alumel type. It is connected to a Leeds and Northrup potentiometer pyrometer indicating temperature in the test chamber. Also on the control panel is an AC ammeter indicating furnace current. Furnace current, and therefore, the rate of temperature rise, is controlled by a rheostat control.

Young's Modulus Measurement Equipment

A dynamic method of determining Young's modulus is afforded by measuring the velocity of sound in glass, which is connected with Young's modulus by the relation:

$$\text{Longitudinal Velocity} = \sqrt{E/d} \qquad (5)$$

in which d is the density and E is Young's modulus. Therefore, in measuring Young's modulus, the main problem is obtaining the velocity of sound through the glass.

In this work, the specimen consisted of a glass fiber of the desired composition which was drawn from the molten glass at the end of a pyrex rod. If a signal of known frequency is applied to the fiber specimen, the velocity of the sound traveling through the specimen can be calculated if the wavelength can be determined by the relation:

$$\text{velocity} = \text{wavelength} \times \text{frequency} \qquad (6)$$

The known frequency is supplied by a Hewlett-Packard model 200 CD Audio

Oscillator whose signal is fed into an Astatic model M-41 transducer which is mounted on an optical bench. Transmission of the input frequency along the optical bench could be minimized by mounting the driving transducer separately. The needle of the transducer was removed and replaced by a two in. piece of piano wire. The transducer received the signal from the oscillator and converted this to mechanical vibrations by use of a piezo-electric material. The transducer was mounted in such a way that the vibrations produced were in a longitudinal direction in relation to the test apparatus. In most cases a frequency of 7,500 cycles was used. One end of the fiber was cemented to the piano wire and the other end to a brass holder, which was also mounted on the optical bench. The holder could be moved backward by use of a screw mechanism till the fiber was taut. When the oscillator was turned on, a standing wave was produced in the fiber in a longitudinal direction.

A phonograph pickup, Astatic Model 312T, with a small brass "V" notch cemented to the needle was used to detect node points along the fiber length, Figure 4. The signal from the pickup was amplified by a Hewlett-Packard Model 400C Vacuum Tube Voltmeter, which is capable of functioning as an amplifier. Amplifications available were 10, 20, 30, 40, 50, 60 db. An Eico Model 460 DC - Wide Band Oscilloscope with the pickup signal as the vertical input and a signal from the audio oscillator as the horizontal input,produced a Lissajous ellipse. When the phonograph pickup passes through a node, the ellipse changes polarity. The Lissajous ellipse is a fundamental pattern obtained when both the vertical and horizontal scope deflection voltages are sinewaves. The patterns are called Lissajous figures after the 19th century French scientist. The

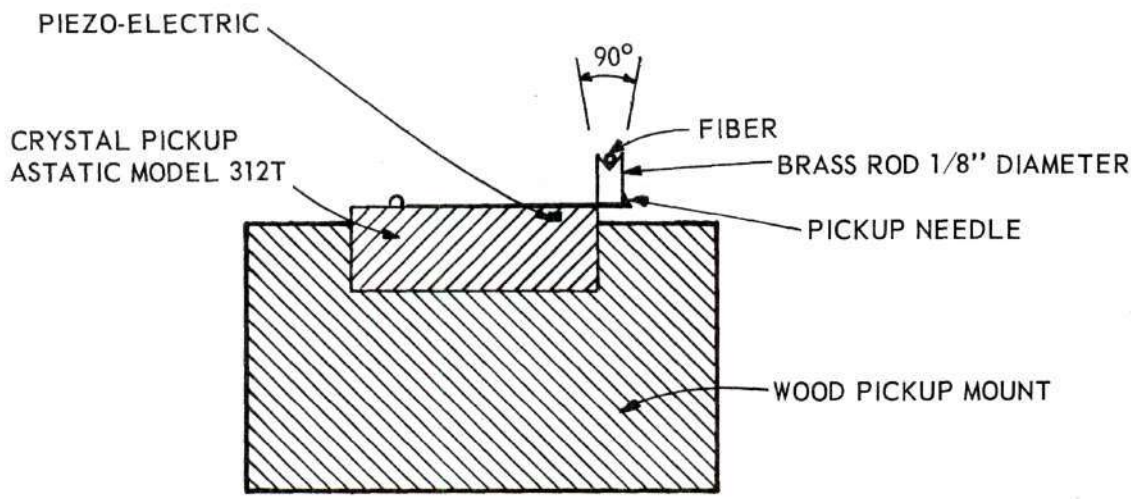

Figure 4. Section View of Phonograph Pickup.

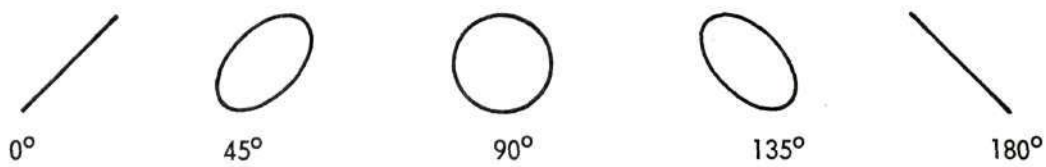

Figure 5. Lissajous Ellipses.

shape of the pattern changes with the phase relationship between the known and unknown signals. The scope patterns and their phase differences are shown in Figure 5.

The pickup was moved along the optical bench until points were found which were 180° apart. This distance is measured by use of a scale divided into one-tenth centimeter graduations mounted along the bench. This then is the half wave length distance, usually between 22 and 27 cm., and two times this figure gives the wavelength. Therefore, the wavelength times the frequency is the velocity of sound through the fiber, which is a fundamental constant of the test specimen. Density of the glass was determined by a picnometer. A photograph of the apparatus is shown in Figure 6.

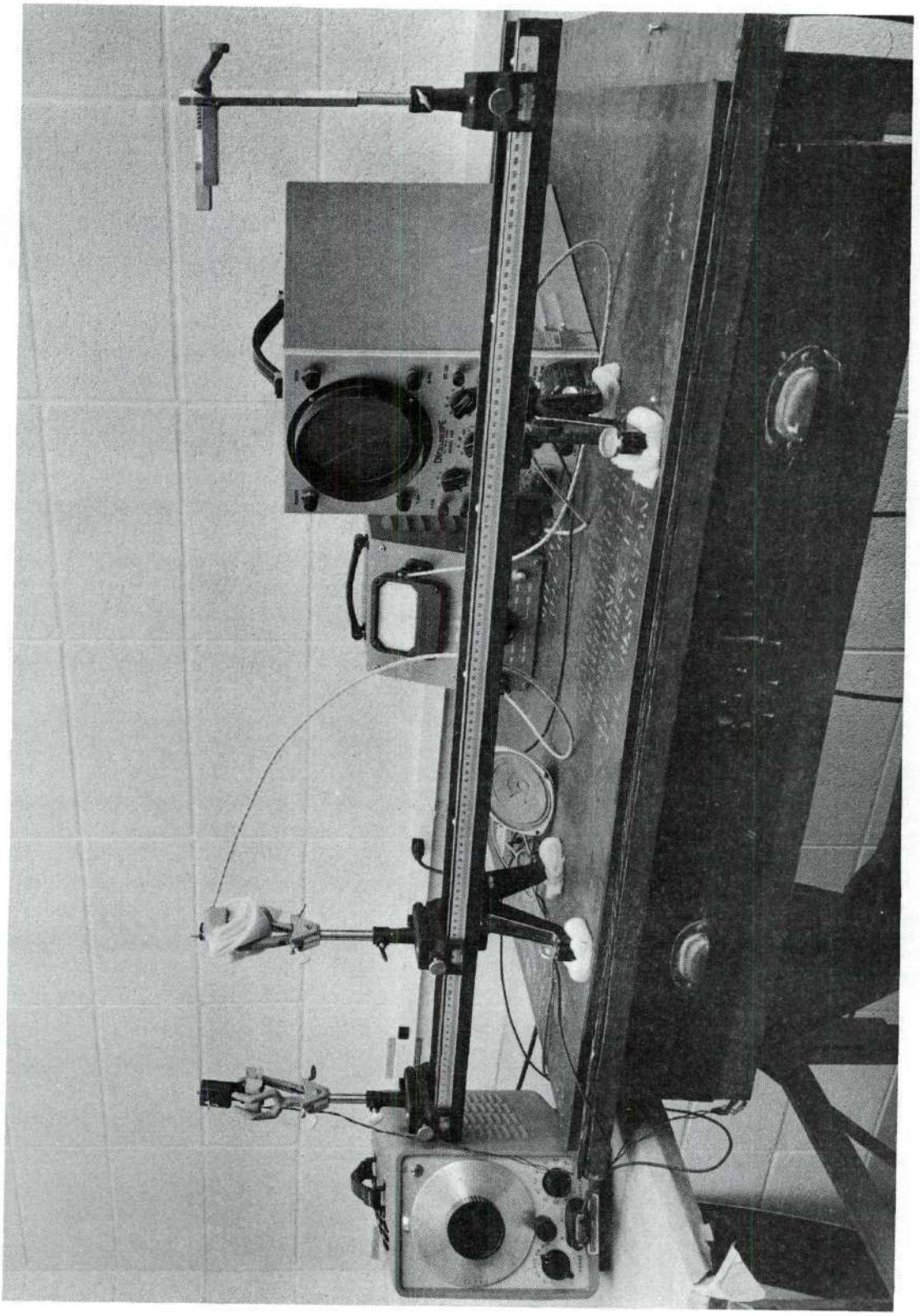

Figure 6. Young's Modulus Measurement Equipment.

CHAPTER IV

PROCEDURE

Composition Selection

The glasses studied had compositions in the range:

1 PbO	0-0.375 B_2O_3	1.0 - 2.0 SiO_2
	0-0.200 Al_2O_3	0 - 0.200 TiO_2
		0 - 0.200 ZrO_2

For each of the two properties, i.e., Young's modulus and thermal expansion, two statistical experimental designs were employed in selecting which compositions to study. All designs used were of the factorial variety so interactions if present could be discovered. Design One, for the coefficient of thermal expansion, was a 4 x 3 x 2 design requiring 24 glass compositions. Lead oxide in these glasses was held constant at one equivalent. Boron content was divided into four equally spaced levels of concentration between 0 and 0.375 equivalents. Silica content was divided into three equally spaced levels of concentration between 1.0 and 2.0 equivalents. This gave compositions one through 12, see Appendix A. The experiment was replicated twice, thus 24 glasses were required. The same design, Design Three, was used for Young's modulus for these same compositions.

For the remainder of the investigation, a 1/3 replicate of a 3^5 design was chosen for each of the two properties, thermal expansion and

Young's modulus, Table 2. Design Two was the design for the coefficient of thermal expansion, and Design Four was for the study of Young's modulus. The five variables, B_2O_3, Al_2O_3, SiO_2, TiO_2, and ZrO_2, were investigated in the ranges specified at three equally spaced levels of concentration. Lead oxide was again held constant at one equivalent. In this case, however, the boron concentration was varied between 0 and 0.250 in three equally spaced levels. A 3^5 design would require 243 glasses, and a 1/3 replicate of a 3^5 design requires only 81 glasses. The particular 81 glasses used must be selected in a definitely prescribed manner. The 81 compositions selected can be seen in Table 2 where a number denotes a composition selected for making a glass. The design was not replicated.

Specimen Preparation

The glass compositions in Appendix A and Table 2 were obtained by combining normal ceramic oxides that gave desirable melting characteristics. Lead oxide was introduced as red lead, lead monosilicate, and lead zirconium silicate. The source of boron was boric acid, titania came from titanium dioxide, and alumina was introduced as aluminum hydroxide. Any deficiency of silica was resolved by the addition of flint.

Batches were weighed on an Ohaus scale capable of weighing to a tenth of a gram. The completed batch was then screened through a 20 mesh screen to break up any lumps. Mixing was accomplished on a large piece of paper which was moved to and fro until the batch looked uniformly pink, showing good dispersion of the red lead, the only highly colored raw material. Contents of the paper were loaded into Denver Fire Clay crucibles five

Table 2. One-third Replicate of 3^5 Design

				B_1 1.0 SiO_2			B_2 1.5 SiO_2			B_3 2.0 SiO_2		
				A_1 0 B_2O_3	A_2 .125 B_2O_3	A_3 .250 B_2O_3	A_1 0 B_2O_3	A_2 .125 B_2O_3	A_3 .250 B_2O_3	A_1 0 B_2O_3	A_2 .125 B_2O_3	A_3 .250 B_2O_3
C_1 0 Al_2O_3	D_1 0 TiO_2	E_1 0 ZrO_2		1					7		8	
		E_2 .100 ZrO_2				13		14		15		
		E_3 .200 ZrO_2			16		17					18
	D_2 .100 TiO_2	E_1 0 ZrO_2				19		20		21		
		E_2 .100 ZrO_2			22		23					24
		E_3 .200 ZrO_2		25					26		27	
	D_3 .200 TiO_2	E_1 0 ZrO_2			28		29					30
		E_2 .100 ZrO_2		31					32		33	
		E_3 .200 ZrO_2				34		35		36		
C_2 .100 Al_2O_3	D_1 0 TiO_2	E_1 0 ZrO_2				37		38		39		
		E_2 .100 ZrO_2			40		41					42
		E_3 .200 ZrO_2		43					44		45	
	D_2 .100 TiO_2	E_1 0 ZrO_2			46		47					48
		E_2 .100 ZrO_2		49					50		51	
		E_3 .200 ZrO_2				52		53		54		
	D_3 .200 TiO_2	E_1 0 ZrO_2		55					56		57	
		E_2 .100 ZrO_2				58		59		60		
		E_3 .200 ZrO_2			61		62					63
C_3 .200 Al_2O_3	D_1 0 TiO_2	E_1 0 ZrO_2			64		65					66
		E_2 .100 ZrO_2		67					68		69	
		E_3 .200 ZrO_2				70		71		72		
	D_2 .100 TiO_2	E_1 0 ZrO_2		73					74		75	
		E_2 .100 ZrO_2				76		77		78		
		E_3 .200 ZrO_2			79		80					81
	D_3 .200 TiO_2	E_1 0 ZrO_2				82		83		84		
		E_2 .100 ZrO_2			85		86					87
		E_3 .200 ZrO_2		88					89		90	

in. high by 3-1/4 in. in diameter.

Filled crucibles were placed in the induction furnace and the furnace turned on. Crucibles were covered in all cases to prevent volatilization of lead. After between one-half and one hour had elapsed, depending on batch composition, the contents were molten. A pyrex rod was dipped into the crucible. If the molten glass from the crucible could be drawn into a smooth fiber, the glass was considered well smelted. If the fiber obtained was rough, i.e., containing seeds, the melt was heated until a smooth fiber was obtained. Compositions number 45, 54, 61, 62, 71, 72, and 79 could not be melted in fireclay in the induction furnace, as the heat required to dissolve all the ingredients was too high. These compositions were successfully melted in a gas fired pot furnace in the fireclay crucibles. Compositions 43, 80, and 89 had to be melted in Norton alumina crucibles in the induction furnace setup. For thermal expansion, a specimen 1/2 by 2 to 3 in. was required. The glass was cast in graphite molds. Graphite blocks approximately 3 x 3 x 1 were used. These blocks had three 1/2 in. diameter holes drilled and reamed through the long dimension. At the start of batch melting, the mold was placed in an electrically heated furnace which was raised to a temperature of 427°C. When the glass melt was ready for casting, the molds were removed from the furnace and placed on a thick slab of steel to seal the bottom. Molten glass was then poured into all three positions of the mold. The remaining melt was poured onto a thick graphite slab to be used later for fiber drawing. Hot molds and contained glass were then placed in the electric furnace, which was turned off, and allowed to cool to room temperature overnight. The glass specimens were removed from the mold by forcing a rod through the

opening. The glass specimen from the graphite slab was carefully inspected for undissolved material. If it was satisfactory, it was remelted in a Denver Fire Clay Crucible 3 in. high by 2-1/4 in. in diameter. When this was thoroughly melted a pyrex glass rod was dipped into the melt. The rod was withdrawn with some of the glass adhering to it. By jerking the rod, a small bead of glass fell from it, pulling a fiber along with it. This fiber was then stretched by grasping the fiber in one hand and the rod in the other and pulling the hands apart at as constant a rate as possible. The fiber was broken away from the glass and inspected for seeds. If no seeds were apparent in at least a 40 in. span, the specimen was placed in a clothespin and saved for testing. Generally, about ten fibers were collected from each melt.

When the fiber drawing apparatus was used, the glass specimen from the graphite slab was loaded into the platinum crucible and the induction furnace turned on. The crucible temperature was increased slowly to the drawing temperature, between 750°C. and 900°C., depending on the composition being melted. The desired temperature was the point at which the viscosity of the glass was low enough to flow slowly through the 0.035 in. orifice, but not so low that it ran freely through. When a small quantity of glass formed on the outside of the bushing, it was pulled away with a small platinum wire, pulling a fiber along with it. This fiber was put through the thread guide and taped to the plexiglas drum. The thread guide was set to run along the length of the drum about ten times per minute. The speed of the drum was regulated such that glass was pulled away from the orifice as soon as it collected there. Usual speeds ranged from 60 to 140 rpm. Once the correct drawing temperature was reached,

and drum rotation speed set, continuous fibers could be drawn for hours.

Coefficient of Thermal Expansion

When the cylindrical specimens were removed from the mold, the ends were cut off with a diamond saw to remove the irregular ends. The ends were then ground flat and parallel with a Buehler Surfmet Grinder employing a 200 mesh silicon carbide grit belt. The specimen to be ground was placed in a brass tube with a 17/32 in. bore. This was suspended over the belt grinder on an aluminum jig holding the specimen perpendicular to the belt. With the ends ground flat and parallel, the sample length was measured with a 2 to 3 in. micrometer which was read to three decimal places. This figure was recorded. The specimen was loaded into the quartz tube dilatometer and its dial gage was set at zero, initial temperature was read and recorded. The furnace was turned on and the amperage set at 3.5 amps. Readings of time, temperature, amperage, and cumulative expansion were obtained every five minutes. Input amperage to the furnace was raised periodically to maintain about a 25 to 30°C. temperature rise per five minute interval. Data was obtained for each specimen from room temperature to the softening point of the glass. From the temperature versus cumulative expansion data, linear regression, Appendix B, was employed to find the slope of the best fit straight line. The linear coefficient of thermal expansion was then calculated by means of the equation:

$$\alpha = \frac{\text{Slope of the regression line}}{\text{Original length of specimen}} + .54 \times 10^{-6} \qquad (7)$$

The last term in this equation is the correction factor for the expansion

of the quartz tube.

Coefficient of expansion values were then assembled into the proper design charts. For compositions 1 through 12 two completely separate runs were made for each batch from weighing and smelting to measurement of expansion. For the compositions in Design Three, only one specimen was made. The data was analyzed by means of the Analysis of Variance technique, Appendices C and E, to discover the significant main effects and two factor interactions. These data were further analyzed with the help of other appropriate statistical techniques. Finally, by use of a Burrough's B-5000 computer and a multiple regression program, Appendix D, equations were developed to fit the data, expressing the coefficient of thermal expansion in the regions of composition studied.

Young's Modulus

A uniform diameter fiber was selected for each composition and cemented to the drive transducer on the Young's modulus test equipment and pulled taut. Generally, a frequency of 7,500 cycles was sent through the fiber, but in some cases a frequency of 15,000 cycles was used. The equipment was more sensitive at 7,500 cycles than at the recommended 15,000 cycles. The pickup was moved along the fiber until the pattern on the oscilloscope was a diagonal line. Centimeter scale reading of this point was recorded as node one. Then the pickup was moved further down the line until the scope showed a pattern 180° out of phase from node one. This was recorded as node two. This procedure was repeated until four node points were located. From the data, the average wavelength was calculated. Velocity of sound through a fiber is equal to the average wavelength times the frequency used.

Density of the particular glass used was found by the picnometer method. A specimen of the glass was ground up in a morter until it was relatively fine and would fit through the narrow mouth of the picnometer. The empty picnometer was weighed on a Mettler balance and recorded. Then the picnometer was filled with distilled water and weighed again. Next, about ten grams of glass was loaded into the dried picnometer and weighed again. Finally, the picnometer plus glass was filled with distilled water and weighed. The density was then equal to:

$$E = \frac{w - p}{(w - p) - (w_2 - w_1)} \tag{8}$$

where D = density;

w = weight of the stoppered picnometer and sample;

p = weight of the stoppered picnometer;

w_1 = weight of the stoppered picnometer filled with water;

w_2 = weight of the stoppered picnometer, sample and water.

Young's modulus was then calculated from the equation:

$$E = \text{Velocity}^2 \times \text{density} \tag{9}$$

For compositions 1 through 12, two completely separate runs were made from batch weighing and smelting to measurement. On all the other compositions, only one fiber was tested unless there was some doubt concerning the data. In this case, a second fiber from the same melt was measured, and the one that had the most repeatable node distances was reported. Young's modulus data was collected and analyzed, Design Two and Four, by the same procedures used for the coefficient of expansion, Designs One and Three.

CHAPTER V

DISCUSSION OF RESULTS

Raw Material Selection

At the temperatures used in the smelting of the glasses, carbon from the induction furnace susceptor had a tendency to diffuse through the fireclay crucible walls causing the glass to turn dark due to reduction of lead oxide. For this reason a portion of the lead content of each batch was made up of red lead. When this compound is heated it gives off oxygen which combines with any free carbon to give off harmless carbon dioxide. About three per cent of the batch was found to be sufficient for this purpose.

Lead monosilicate was selected as the major lead introducing compound. This is a relatively non-poisonous source of lead oxide and is also an aid in melting some of the silica component of the glass. Furthermore, it is a rigidly controlled product as to lead and silica content.

Zirconium oxide was introduced as lead zirconium silicate. Many other zirconia compounds such as zirconium oxide, milled zircon, and Superpax were tried, but none of these would dissolve completely in the glass. Lead zirconium silicate is a solid state combination of lead and zircon which has a much lower melting temperature than zircon alone. At the middle level of the zirconia addition, 0.100 equivalents, the lead zirconium silicate dissolved fairly easily. However, at 0.200 equivalents and low boron contents it could be dissolved completely

only with great difficulty.

Boron additions were made with boric acid. This is the common source of boron when no soda can be tolerated. Titania was added as titanium dioxide, the most common source in ceramics. The alumina was added as aluminum hydroxide, because experiments showed that this source of alumina dissolved easiest in the glass compositions of interest.

Sample Preparation

The induction crucible furnace was designed specifically for this work. Generally, glass is smelted in a gas fired pot furnace. Induction heating has two main advantages over a pot furnace. First, the heat being generated in the induction furnace is only in the graphite susceptor. Therefore, while the pot furnace gives off large amounts of heat to the surrounding room, the induction furnace gives off very little. This is quite important in manipulation and also during removal of the crucible for pouring. The induction furnace makes almost pleasant work out of something that is generally considered an extremely undesirable chore. The second big advantage of induction heating is that the atmosphere is always relatively constant, as there are no combustion products from the furnace. This eliminates something that could be a variable in the experiment.

The one drawback to the furnace used is its inefficiency of heating. Heat is only generated in the graphite susceptor, and this heat has to be transferred first to the clay crucible and then on to the batch. For this reason, to melt some of the batches, especially the ones containing high zirconium oxide, the graphite had to be brought up to very high temperatures to conduct sufficient heat through the crucible to melt the

batch. In some cases this heat was so high that it melted the fireclay crucible, causing loss of the batch. After this happened twice on any particular composition the third trial was carried out in a gas pot furnace where the crucible did not have to be hotter than the batch. Compositions 45, 54, 61, 62, 71, 72, and 79 were successfully smelted in the pot furnace. Even with this procedure, clear glasses of compositions 43, 80, and 89 could not be obtained. These three compositions were smelted in Norton BP-70548 pure alumina crucibles in the induction furnace. These crucibles are capable of withstanding a much higher temperature than fireclay without melting. Another problem encountered in the smelting was that as the graphite susceptors were used they would volitalize and shrink in size. As they became small they would cause the crucibles to crack due to unequal heating. The batch would leak through these fissures and be destroyed. Due to all causes, including those already mentioned, 228 melts were required to obtain the 102 required glass compositions.

At first, obtaining a material to mold the glass in was quite a problem. First trials were made with split-steel molds having circular holes bored in them. When the hot glass came into contact with the cold molds, the glass would solidify rapidly and only short irregular shapes of glass were obtained. When these molds were heated to prevent this, the glass adhered to the mold faces and the specimens could not be removed. A graphite grease was applied to the heated mold faces, but this volitalized and either gave defective casts if the glass was poured immediately after application, or would not prevent adhering if time was allowed for volitalization to cease. Several other configurations of steel molds were tried, but none were successful.

Some ceramic kiln posts were found that had a hole in them 1/2 in. in diameter and were available in three in. lengths. When the hot glass was poured into these molds they would generally hold together until the glass solidified, and then would crack open due to the thermal shock. These molds worked quite well for the first few compositions tried, generally about one out of every three bars cast was acceptable. However, when some of the more refractory compositions were tried they adhered to the mold surfaces and could not be used. After trials with heated molds, which aggrevated the problem, and graphite greased molds, this technique was abandoned.

Finally, graphite molds were tried. The molds were extremely simple to make, last for a number of casts, and the graphite is relatively low priced. A three in. graphite block was obtained and three 15/32 in. holes drilled through it. These holes were then reamed to 1/2 in. Drilling was done in a lathe to assure a perfectly straight hole. From the first, these molds were highly successful. After a mold had been used several times, the inside faces became scarred, producing rough bars, and eventually after several more runs the bars could not be freed from the mold. The molds were then discarded and replaced by new ones.

Early in the work it became apparent that if the glasses were cooled too rapidly they would crack. After some experimentation it was decided that if the compositions were annealed from 427°C. down to room temperature this difficulty was overcome. All glasses were given approximately the same heat treatment of annealing from 427°C. If the glasses containing the high levels of zirconium and/or titanium were allowed to cool slowly from smelting temperature to annealing temperature, crystalli-

zation of these ingredients would occur. Therefore, the annealing temperature of 427°C. was desirable, as the rapid quench of the glasses to 427°C. was sufficient to lock in the structure and prevent crystallization, yet not so low as to cause high strains.

The sonic determination of Young's modulus requires perfectly melted glasses with no discontinuities. This fact makes it desirable to draw a continuous fiber from a standard diameter bushing. The fiber apparatus worked very well in the preliminary runs. Excellent continuous fiber was drawn for periods up to two hours. However, when compositions containing zircon and/or titania were tried, difficulties were encountered. When proper drawing temperatures for these compositions were maintained, crystallization of the zircon and/or titania would ensue after a relatively short period. This rendered the fibers useless due to seeds. When the temperature of the melt was raised high enough to remelt these seeds, the viscosity of the melt was so low that a continuous fiber could not be drawn. Therefore, this apparatus was abandoned for all compositions to eliminate the variable of drawing method and all fibers used were hand drawn, as explained in the procedure.

Hand drawn fibers are not nearly as desirable as mechanically drawn fibers, because of their lack of uniformity in diameter. With the glass compositions studied there was no other choice available. Generally, a remarkably constant diameter fiber could be drawn by hand. However, there were always slight variations in these fibers which the sonic apparatus never failed to detect. Results were good enough with these fibers to continue the work using them.

In general, each of the ingredient additions caused some physical

changes in the glass other than the two properties under consideration. Titania additions to the basic lead-monosilicate glass caused it to turn brown. The higher the titania addition, the browner the glass. The titania additions did not have any noticeable effect on the viscosity of the melted glass, and very little effect on the temperature required to smelt it. Alumina additions only seemed to effect the smelting temperature of the glass, making it somewhat more refractory. Silica additions made the melted glass considerably more viscose and increased the melting temperature. Boron was quite effective in reducing the viscosity of the melts, and had a small effect in reducing melting temperature. In the compositions where zircon was used, the boron was extremely helpful in dissolving the lead zirconium silicate. All the troublesome batches had high zirconia content and none or the lower level of boron content. The zirconia additions materially increased the smelting temperatures and the viscosity of the melt. All high zirconia and high titania batches were dark brown in color. Zirconia darkened all glasses to some extent, especially at the highest level of concentration.

Coefficient of Thermal Expansion

Several couples were inserted into the inner quartz tube, one at the base of the tube, one one in. above the base, one three in. above the base, and one five in. above the base. The two couples nearest the base checked out at ±9°C. over the range 20°C. to 600°C. with the instrument thermocouple. The two highest thermocouples were consistently 8° to 15°C. lower than the instrument couple. However, since the maximum specimen length was less than three in., the instrument thermocouple was considered

to be an accurate measure of the temperature. Generally the greatest disagreement between the couples was in the initial heating where there was a temperature lag inside the tube. As a test of the system as a whole, a sample rod of lead bisilicate was made. The value obtained for the coefficient of expansion of this rod was 7.18×10^{-6} in./in./°C., as compared with the commonly accepted value for this composition of 7.10×10^{-6} in./in./°C.

The expansion curves for all the glass compositions showed similar characteristics. During the first 25° to 50°C. of heating, the expansion of the specimens was quite small. This was probably due to the time it took the heat to penetrate through the quartz tube and the start of specimen heating. From this point on the temperature vs. cumulative expansion curve was quite linear up to between 400° and 600°C., depending upon the particular glass composition. When the curve broke from linearity the trend was to a sharply increased expansion rate. This break from linearity is called the transformation temperature or range of the glass, and is a well documented phenomenon in lead-boro-silicate glasses (42). It is the temperature region over which the transformation occurs from the glassy to the super-cooled state, and vice versa. The transformation region for the glasses in this study were between 35° and 75°C. After this period, the expansion of the rod seemed to cease for a period of about 25°C. and then started to drop rapidly, indicating that the specimen had reached its softening temperature.

The statistical procedure of linear regression was used to find the slope of the best fit line to the temperature vs. cumulative expansion data between room temperature and the transformation temperature for each composition. An example of this type of calculation can be found in

Appendix B. This is a highly valid technique for determining the coefficient of expansion, because the specimens expand at a nearly constant rate in this region. Any small deviations from linearity are in all probability due to experimental error or time lag in heating the specimen.

Design One

Design One was the 4 x 3 x 2 factorial design for the coefficient of thermal expansion. The values obtained by linear regression for the coefficient of thermal expansion are given in Table 3. Since two completely separate runs from weighing and smelting to expansion measurement were obtained, there are two readings per box.

The data were analyzed by the analysis of variance technique. The completed analysis of variance table is seen in Table 4. The details of the calculation and interpretation of this table appear as Appendix C. From the analysis of variance several important facts can be uncovered. The best estimate of the standard deviation due to experimental error, σ_o, for this experiment is 0.1658×10^{-6} in./in./°C. This value represents about 1.8 per cent of the values obtained for the coefficient of thermal expansion. With 90 per cent confidence, the true value of the standard deviation due to experimental error lies in the range 0.1253×10^{-6} to 0.2512×10^{-6} to 0.2512×10^{-6} in./in./°C.

The boron-silica interaction was significant. This interaction is mainly due to the fact that the effect of boron on the coefficient of thermal expansion varies at different levels of the silica concentration. At 1.0 and 2.0 equivalents of silica boron in all probability cause a decrease in the thermal expansion of the glass. The higher the boron content the

Table 3. Coefficient of Thermal Expansion x 10^6 in./in./°C. Design One

Lead Oxide Held Constant at 1.0 Equivalent

Factor A - B_2O_3

Factor B - SiO_2	Level A_1 0 Equiv. B_2O_3	Level A_2 0.125 Equiv. B_2O_3	Level A_3 0.250 Equiv. B_2O_3	Level A_4 0.375 Equiv. B_2O_3	Total
Level B_1 1.0 Equiv. SiO_2	10.67 10.96	10.31 10.51	10.15 9.92	10.21 10.05	82.78
Level B_2 1.5 Equiv. SiO_2	8.84 8.92	8.55 8.58	8.78 8.90	8.83 8.53	69.93
Level B_3 2.0 Equiv. SiO_2	7.84 7.53	7.98 7.74	7.43 7.01	7.38 7.26	60.17
Total	54.76	53.67	52.19	52.26	212.88

lower the thermal expansion up to 0.250 equivalents. However, at 0.375 equivalents this trend ceases, and boron does not reduce the coefficient of expansion further. At 1.5 equivalents of silica, varying the boron has in all probability no effect on the coefficient of expansion. Any differences in the values are probably due to experimental error.

The effect of silica in all cases was a substantial lowering of the

coefficient of thermal expansion. The effect of this factor was significantly greater than the other effects in this experiment. Silica seemed to have about the same lowering effect on the thermal expansion regardless of the level of boron, with the small deviations from this trend being due entirely to experimental error.

With the help of the Burroughs B-5000 computer, and a multiple regression analysis program, equations representing the linear coefficient of thermal expansion in this region of compositions was developed. Details of this program are in Appendix D. The process employed related the dependent variable, coefficient of thermal expansion, to the independent variables boron and silica content. The six regression equations tried are seen in Table 5. Model number two, the cross product model, was judged the best fit because for eight of the twelve glass compositions the calculated value from this equation fell between the two experimental values for the composition. This model also had the lowest standard error of estimate.

Table 4. Analysis of Variance Design One

Effect	Sum of Squares	Degrees of Freedom	Mean Square	F Ratio
Boron	0.7594	3	0.2531	9.20
Silica	32.1497	2	16.0739	583.51
Boron and Silica Int.	0.6487	6	0.1081	3.93
Experimental Error	0.3294	12	0.0275	----
Total	33.8872	23	----	----

Table 5. Coefficient of Thermal Expansion

Equations Design One

Composition Limits:	1 PbO
	0 - 0.375 B_2O_3
	1.0 - 2.0 SiO_2

X_1 = equiv. B_2O_3 X_2 = equiv. SiO_2

1. Model: Linear

$\alpha = A_o \pm A_1X_1 \pm A_2X_2$

$\alpha = 13.33 \times 10^{-6} - 1.20 \times 10^{-6} X_1 - 2.83 \times 10^{-6} X_2$

Std. error est. = 2.45×10^{-7} in./in./°C.

2. Model: Cross Product (Best Fit)

$\alpha = A_o \pm A_1X_1 \pm A_2X_2 \pm A_3X_1X_2$

$\alpha = 13.48 \times 10^{-6} - 2.10 \times 10^{-6} X_1 - 2.92 \times 10^{-6} X_2 + 6.36 \times 10^{-7} X_1X_2$

Std. error est. = 2.33×10^{-7} in./in./°C.

3. Model: One Over Cross Product

$\alpha = A_o \pm A_1X_1 \pm A_2X_2 \pm A_3/X_1X_2$

$\alpha = 13.12 \times 10^{-6} - 7.40 \times 10^{-9} X_1 - 2.68 \times 10^{-6} X_2 - 6.51 \times 10^{-7}/X_1X_2$

Std. error est. = 2.47×10^{-7} in./in./°C.

(Continued)

Table 5 (Continued)

4. Model: Square Term

$$\alpha = A_o \pm A_1X \pm A_2X_2 \pm A_3X_1^2$$

$$\alpha = 13.32 \times 10^{-6} + 2.29 \times 10^{-6} X_1 - 2.79 \times 10^{-6} X_2 - 2.02 \times 10^{-6} X_1^2$$

Std. error est. = 2.34×10^{-7} in./in./°C.

5. Model: One Over Square Term

$$\alpha = A_o \pm A_1X_1 \pm A_2X_2 \pm A_3/X_1^2$$

$$\alpha = 13.31 \times 10^{-6} - 9.06 \times 10^{-8} X_1 - 2.79 \times 10^{-6} X_2 - 9.40/X_1^2$$

Std. error est. = 2.35×10^{-7} in./in./°C.

6. Model: One Over Term

$$\alpha = A_o \pm A_1X_1 \pm A_2X_2 \pm A_3/X_1$$

$$\alpha = 13.30 \times 10^{-6} - 6.37 \times 10^{-9} X_1 - 2.79 \times 10^{-6} X_2 - 1.14 \times 10^{-6}/X_1$$

Std. error est. = 2.36×10^{-7} in./in./°C.

Design Two

Design two was the 1/3 replicate of the 3^5 design for the investigation of the changes produced on the thermal expansion by additions of silica, boron, alumina, titania, and zirconia to the lead glass. Factor A was boron content, B silica content, C alumina, D titania, and E the zirconia content. The values for the linear coefficient of thermal expansion comprise Table 6. The data were analyzed by the analysis of variance technique, Appendix E. Table 7 is the completed ANOVA table for this design.

Table 6. Coefficient of Thermal Expansion x 10^6 in./in./°C. Design Two

Lead Oxide Held Constant at 1.0 Equivalent

			B_1 1.0 SiO_2			B_2 1.5 SiO_2			B_3 2.0 SiO_2		
			A_1 0 B_2O_3	A_2 .125 B_2O_3	A_3 .250 B_2O_3	A_1 0 B_2O_3	A_2 .125 B_2O_3	A_3 .250 B_2O_3	A_i 0 B_2O_3	A_2 .125 B_2O_3	A_3 .250 B_2O_3
C_1 0 Al_2O_3	D_1 0 TiO_2	E_1 0 ZrO_2	10.82					8.84		7.86	
		E_2 .100 ZrO_2			10.04		8.21		6.84		
		E_3 .200 ZrO_2		18.18		7.33					6.49
	D_2 .100 TiO_2	E_1 0 ZrO_2			10.37		9.28		7.93		
		E_2 .100 ZrO_2		9.23		7.94					7.25
		E_3 .200 ZrO_2	7.83					7.67		6.70	
	D_3 .200 TiO_2	E_1 0 ZrO_2		9.88		9.29					7.86
		E_2 .100 ZrO_2	9.17					8.11		7.12	
		E_3 .200 ZrO_2			8.63		7.85		6.62		
C_2 .100 Al_2O_3	D_1 0 TiO_2	E_1 0 ZrO_2			10.08		8.33		7.23		
		E_2 .100 ZrO_2		7.72		7.56					7.10
		E_3 .200 ZrO_2	7.28					6.80		6.10	
	D_2 .100 TiO_2	E_1 0 ZrO_2		9.99		8.20					8.13
		E_2 .100 ZrO_2	8.14					7.52		6.76	
		E_3 .200 ZrO_2			7.02		6.70		6.28		
	D_3 .200 TiO_2	E_1 0 ZrO_2	9.68					8.43		7.50	
		E_2 .100 ZrO_2			8.58		7.66		6.74		
		E_3 .200 ZrO_2		7.43		7.04					6.33
C_3 .200 Al_2O_3	D_1 0 TiO_2	E_1 0 ZrO_2		9.55		8.14					7.39
		E_2 .100 ZrO_2	6.76					6.68		6.44	
		E_3 .200 ZrO_2			6.61		6.45		6.15		
	D_2 .100 TiO_2	E_1 0 ZrO_2	9.06					8.11		7.50	
		E_2 .100 ZrO_2			7.87		7.03		6.68		
		E_3 .200 ZrO_2		7.21		6.84					6.57
	D_3 .200 TiO_2	E_1 0 ZrO_2			8.71		7.95		7.20		
		E_2 .100 ZrO_2		7.66		6.95					6.61
		E_3 .200 ZrO_2	6.80					6.40		6.07	

Table 7. ANOVA Coefficient of Thermal Expansion

Design Two

Effect	Sum of Squares	Degrees of Freedom	Mean Square	F Ratio	Comments
A	0.25352	2	0.12676	1.504	Not sign.
B	34.06274	2	17.08137	202.698	Sign. at .01 level
C	14.69415	2	7.34708	87.185	Sign. at .01 level
D	0.14870	2	0.07435	0.882	Not sign.
E	39.94751	2	19.97376	237.021	Sign. at .01 level
AB	0.37755	4	0.09439	1.120	Not sign.
AC	0.21481	4	0.05370	0.637	Not sign.
AD	0.15192	4	0.03798	0.451	Not sign.
AE	0.27822	4	0.06956	0.825	Not sign.
BC	2.76874	4	0.69219	8.214	Sign. at .01 level
BD	0.27130	4	0.06783	0.805	Not sign.
BE	3.01549	4	0.75387	8.946	Sign. at .01 level
CD	0.44709	4	0.11177	1.326	Not sign.
CE	0.47186	4	0.11797	1.399	Not sign.
DE	0.42527	4	0.10132	1.202	Not sign.
Residual	2.52820	30	0.08427	---	---
Total	100.05707	80	---	---	---

A 1/3 replicate of a full factorial design cannot be expected to give as much information as the full factorial design. In the design chosen, only the main effects and the two factor interactions can be analyzed. The higher order interactions remain in the residual term and expand it. Some fraction of the rest of the higher order interaction terms are confounded with the main effects and the two factor interactions. The variance of the residual term was 0.08427×10^{-12}, and the standard deviation was 0.2901×10^{-6} in./in./°C. This is comparable to the standard deviation in Design One of 0.1658×10^{-6} in./in./°C., which was due entirely to experimental error. Most of the difference between these two values is due to the high order interactions. Thus the higher order interactions probably would not make a difference of over two per cent in the value obtained for the coefficient of expansion of any sample. Furthermore, the confounded interactions, in all probability, would be only a small fraction of this value, and would have only a very slight effect on the mean square values obtained for the main effects and two factor interactions.

Some of the sensitivity of the test is lost by adding the experimental error together with the high order interactions, forming the residual term which is the term that all the other effects are tested against. However, since the residual term in this experiment was relatively small, all major effects are locatable.

It turns out that the only significant effects in this experiment are those of silica, alumina, zirconia, silica-alumina interaction, and the silica-zirconia interaction. None of the other factors could have had an effect of over 3.7 percent on the thermal expansion. Thus this design analyzed all major effects and missed only minor effects with 1/3 the normal amount of experimentation.

In general, silica additions decrease the coefficient of thermal expansion. Boron and titania have very little or no effect on the coefficient of thermal expansion. Zirconia and alumina additions both produce a marked lowering of the coefficient of expansion. In ranked order, zirconia was probably the most effective in reducing thermal expansion, followed quite closely by silica, and somewhat further behind was alumina. The two interactions noted in this work, silica-alumina, and silica-zirconia, were a deminishing of the effect of silica in decreasing the thermal expansion at the higher levels of zirconia and alumina, and a decreasing of the effectiveness of zirconia and alumina at high levels of silica. In other words, as the coefficient of thermal expansion decreases, further additions of silica, alumina, or zirconia have less and less effect in decreasing the expansion.

Equations were developed to express the coefficient of thermal expansion in this region by use of the multiple regression procedure. These equations are listed in Table 8.

Table 8. Coefficient of Thermal Expansion Equations

Design Two

Composition Limits		
1.0 PbO	0 - 0.250 B_2O_3	1.0 - 2.0 SiO_2
	0 - 0.200 Al_2O_3	0 - 0.200 TiO_2
		0 - 0.200 ZrO_2
X_1 = equiv. B_2O_3	X_2 = equivl SiO_2	
X_3 = equiv. Al_2O_3	X_4 = equiv. TiO_2	
X_5 = equiv. ZrO_2		

(Continued)

Table 8. (Continued)

1. Model: Linear

$$\alpha = Ao \pm A_1X_1 \pm A_2X_2 \pm A_3X_3 \pm A_4X_4 \pm A_5X_5$$

$$\alpha = 11.37 \times 10^{-6} + 0.55 \times 10^{-6} X_1 - 1.59 \times 10^{-6} X_2 - 5.18 \times 10^{-6} X_3 + 0.24 \times 10^{-6} X_4 - 8.51 \times 10^{-6} X_5$$

Std. error est. = 4.06×10^{-7} in./in./°C.

2. Model: Silica-Zirconium Interaction

$$\alpha = Ao \pm A_1X_1 \pm A_2X_2 \pm A_3X_3 \pm A_4X_4 \pm A_5X_5 \pm A_6/X_2X_5$$

$$\alpha = 11.70 \times 10^{-6} + 0.55 \times 10^{-6} X_1 - 1.72 \times 10^{-6} X_2 - 5.18 \times 10^{-6} X_3 + 0.24 \times 10^{-6} X_4 - 7.77 \times 10^{-6} X_5 - 0.05 \times 10^{-6}/X_2X_5$$

Std. error est. = 3.86×10^{-7} in./in./°C.

3. Model: Silica-Alumina Interaction

$$\alpha = Ao \pm A_1X_1 \pm A_2X_2 \pm A_3X_3 \pm A_4X_4 \pm A_5X_5 \pm A_6/X_2X_3$$

$$\alpha = 11.57 \times 10^{-6} + 0.55 \times 10^{-6} X_1 - 1.67 \times 10^{-6} X_2 - 4.74 \times 10^{-6} X_3 + 0.24 \times 10^{-6} X_4 - 8.51 \times 10^{-6} X_5 - 0.03 \times 10^{-6}/X_2X_3$$

Std. error est. = 4.01×10^{-7} in./in./°C.

4. Model: Silica-Zirconia plus Silica-Alumina Interaction (Best Fit)

$$\alpha = Ao \pm A_1X_1 \pm A_2X_2 \pm A_3X_3 \pm A_4X_4 \pm A_5X_5 \pm A_6/X_2X_3 \pm A_7/X_2X_5$$

$$\alpha = 11.89 \times 10^{-6} + 0.55 \times 10^{-6} X_1 - 1.80 \times 10^{-6} X_2 - 4.75 \times 10^{-6} X_3 + 0.24 \times 10^{-6} X_4 - 7.77 \times 10^{-6} X_5 - 0.03 \times 10^{-6}/X_2X_3 - 0.03 \times 10^{-6}/X_2X_5$$

Std. error est. = 3.80×10^{-7} in./in./°C.

5. Model: Alumina-Titania Interaction

$$\alpha = Ao \pm A_1X_1 \pm A_2X_2 \pm A_3X_3 \pm A_4X_4 \pm A_5X_5 \pm A_6/X_3X_4$$

$$\alpha = 11.37 \times 10^{-6} + 0.55 \times 10^{-6} X_1 - 1.59 \times 10^{-6} X_2 - 5.16 \times 10^{-6} X_3 + 0.25 \times 10^{-6} X_4 - 8.50 \times 10^{-6} X_5 - 0.01 \times 10^{-6}/X_3X_4$$

Std. error est. = 4.09×10^{-7} in./in./°C.

Model equation four was selected as the best fit, due to the fact that it gave the smallest average error over the region studied. The observed coefficient and the calculated coefficient using this equation differed by as much as ten percent for only one case, composition 13. For most other compositions, calculated and observed values differed by less than five per cent. This was only slightly poorer than the estimate of the experimental error and high order interactions in this region. The only way in which a closer fit equation could be developed would be to use equations with more polynomial terms. However, this would make the calculation using these equations tedious and would not reduce the error enough to make it worthwhile.

Young's Modulus

There was some variation in the diameter of the hand drawn fibers. This fact, plus the probability of a small amount of micro-crystalline material in the compositions containing zirconia and/or titania, accounts primarily for the distance between the node points of the fiber not being exactly repetitious. Every discontinuity in the fiber slightly distorts the fibers mode of vibration. Therefore, around the true node points there generally were some other flip frequencies. In most cases these flips were of a much lower intensity and easily discarded. However, these discontinuities in the fiber specimen were enough to vary the observed distance between node points as much as 1.2 cm. This large a deviation could cause the value obtained for Young's modulus to be off by as much as five per cent. The condition was minimized to some extent by using the distances between four node points and averaging them to obtain the wavelength.

The apparatus was calibrated by using a standard Owens-Corning type E fiberglass. The fiber has a known modulus of 10.5×10^6 psi, which calculates to a wavelength of 35.4 cm. at a frequency of 15,000 cycles. When the fiber was tested on the sonic apparatus used in this experiment, the node points were found within one per cent of the expected value. Using the standard commercially drawn fiber, no flips were found except at the expected node points. The standard fiber was used periodically to recheck the apparatus.

Design Three

Design Three was the 4 x 3 x 2 factorial design for the investigation of Young's modulus in the region:

1	PbO	0 - 0.375	B_2O_3	1.0 - 2.0	SiO_2

The values of Young's modulus obtained for the 12 glasses studied in this region comprise Table 9. Table 10 is the completed analysis of variance, and details of this analysis are Appendix F. The best estimate of the experimental-error standard deviation was 10.62 kilobars. This represents an average error of around 2.1 per cent. With 90 per cent confidence, the true value of the standard deviation due to experimental error lies in the range 8.02 to 16.04 kilobars.

All additions to the initial composition, 1.0 PbO plus 1.0 SiO_2, produced an increase in Young's modulus. The higher the Young's modulus, the stronger the bond strength of the structure. However, the higher the Young's modulus, the more brittle the glass, and therefore, it is more prone to crazing. Generally speaking, additions which decrease the

Table 9. Young's Modulus in Kilobars Design Three

Factor B - Equivalents of SiO_2	Factor A - Equivalents of B_2O_3				
	0 B_2O_3	0.125 B_2O_3	0.250 B_2O_3	0.375 B_2O_3	Total
1.0 PbO 1.0 SiO_2	438 445	461 465	471 472	563 570	3,885
1.0 PbO 1.5 SiO_2	483 477	539 530	580 570	562 542	4,283
1.0 PbO 2.0 SiO_2	508 508	522 519	533 525	575 568	4,258
Total	2859	3036	3151	3380	12,426

coefficient of thermal expansion increase the modulus of elasticity for most materials. Thus while all ingredient additions tended to increase Young's modulus, and therefore make the glazes more prone to crazing, the values are still considerably lower than for most glasses. Most glasses have Young's modulus in the region 650 - 800 kilobars (48) or even higher. Thus, all glasses tested would be lower strength but more craze resistant than most glasses in general. This also accounts for the weaker bond energies and low scratch resistance of high lead glazes.

The effects of silica and boron additions are quite variable. At level B_1, 1.0 equivalent of silica, the first two levels of boron, however, a significant increase in Young's modulus is noted. At level

B_3, 2.0 equivalents of silica, the same trend is noted. However, at level B_2, 1.5 equivalents of silica, the Young's modulus increased rapidly with the first two boron additions and then leveled off. Again, level B_2 of the silica addition was different from the other levels of silica additions as it was for the coefficient of thermal expansion. There is most probably some significance in this, as both levels B_1 and B_3 are eutetic mixtures of lead and silica, but level B_2 is not. Since the interaction was so pronounced in this experiment, the level of boron or silica addition must be specified before a prediction of the effect of the other ingredient additions can be made.

Some equations were developed for this design using multiple regression analysis. Since the variability of the effects is relatively large, simple extremely well fitting curves could not be developed from the data. There was a choice available, either develop equations that exactly fit the data, or develop equations which give a reasonable estimate of Young's

Table 10. Young's Modulus ANOVA Design Three

Effect	Sum of Squares	Degrees of Freedom	Mean Square	F Ratio
Boron	23,834.83	3	7,944.94	70.67
Silica	12,423.25	2	6,211.63	55.12
Boron Silica Inter.	8,019.92	6	1,336.65	11.86
Experimental Error	1,352.50	12	112.71	---
Total	45,630.50	23	- - -	---

modulus. If the first choice were made, this would require, in all probability, a 12 degree polynomial. This would surely coincide with all the experimental points, but would still probably be somewhat off on intermediate points, i.e. compositions not run. The large amount of work required to solve the equation for any given composition would in all probability preclude anyone from using it. Therefore, the second choice was made with the full realization that the final equations have a fairly large standard error, but at least give a reasonable estimate of Young's modulus with a minimum of computation. The best equations developed are presented as Table 11. Model equation three was chosen as the best equation due to its lower standard error of estimate, and also because for only one point the observed value and the computed value differed by more than 25 kilobars.

Design Four

This design was the 1/3 replicate of the 3^5 design for the investigation of changes produced in Young's modulus by additions of silica, boron, alumina, titania, and zirconia. Factor A was boron, B silica, C alumina, D titania, and E zirconia. The experimentally obtained values comprise Table 12. The data were analyzed by the analysis of variance technique. Table 13 is the ANOVA table, and details of calculation and interpretation are in Appendix G.

The design was a fairly good choice, as the residual mean square was comparatively small. The best estimate of the experimental-error standard deviation was 11.38 kilobars. With 90 per cent confidence this value could be no larger than 14.50 kilobars or smaller than 9.42 kilobars. Thus, the average error in using the design could not be greater than 2.5 per cent.

Table 11. Young's Modulus Equations Design Three

Composition Limits	1 PbO
	0 - 0.375 B_2O_3
	1.0 - 2.0 SiO_2
X_1 = equiv. B_2O_3	X_2 = equiv. SiO_2

1. Model: Linear

$E = A_o \pm A_1X_1 \pm A_2X_2$

$E = 406 + 224\ X_1 + 47\ X_2$

Std. error est. = 25.3 Kilobars

2. Model: Cross Product

$E = A_o \pm A_1X_1 \pm A_2X_2 \pm A_3X_1X_2$

$E = 364 + 445\ X_1 + 74\ X_2 - 147\ X_1X_2$

Std. error est. = 24.2 Kilobars

3. Model: Square Term (Best Estimate)

$E = A_o \pm A_1X_1 \pm A_2X_2 \pm A_3X_2^2$

$E = 186 + 224\ X_1 + 364\ X_2 - 106\ X_2^2$

Std. error est. = 22.1 Kilobars

4. Model: Square Term

$E = A_o \pm A_1X_1 \pm A_2X_2 \pm A_3X_1^2$

$E = 408 + 172\ X_1 + 47\ X_2 + 139\ X_1^2$

Std. error est. = 25.8 Kilobars

5. Model: One Over Cross Product

$E = A_o \pm A_1X_1 \pm A_2X_2 \pm A_3/X_1X_2$

$E = 411 + 224\ X_1 + 450\ X_2 - 85/X_1X_2$

Std. error est. = 25.9 Kilobars

Table 12. Young's Modulus in Kilobars Design Four

Lead Oxide Held Constant at 1.0 Equivalent

				B_1 1.0 SiO_2			B_2 1.5 SiO_2			B_3 2.0 SiO_2		
				A_1 0 B_2O_3	A_2 .125 B_2O_3	A_3 .250 B_2O_3	A_1 0 B_2O_3	A_2 .125 B_2O_3	A_3 .250 B_2O_3	A_1 0 B_2O_3	A_2 .125 B_2O_3	A_3 .250 B_2O_3
C_1 0 Al_2O_3	D_1 0 TiO_2	E_1 0 ZrO_2		442					575		521	
		E_2 .100 ZrO_2				540		535		515		
		E_3 .200 ZrO_2			568		543					610
	D_2 .100 TiO_2	E_1 0 ZrO_2				577		537		525		
		E_2 .100 ZrO_2			537		520					610
		E_3 .200 ZrO_2		526					634		591	
	D_3 .200 TiO_2	E_1 0 ZrO_2			549		536					577
		E_2 .100 ZrO_2		524					601		575	
		E_3 .200 ZrO_2				620		592		576		
C_2 .100 Al_2O_3	D_1 0 TiO_2	E_1 0 ZrO_2				584		560		548		
		E_2 .100 ZrO_2			546		533					607
		E_3 .200 ZrO_2		544					617		592	
	D_2 .100 TiO_2	E_1 0 ZrO_2			560		550					618
		E_2 .100 ZrO_2		538					603		577	
		E_3 .200 ZrO_2				582		569		563		
	D_3 .200 TiO_2	E_1 0 ZrO_2		546					608		596	
		E_2 .100 ZrO_2				612		584		571		
		E_3 .200 ZrO_2			605		586					595
C_3 .200 Al_2O_3	D_1 0 TiO_2	E_1 0 ZrO_2			567		561					630
		E_2 .100 ZrO_2		556					627		601	
		E_3 .200 ZrO_2				640		616		603		
	D_2 .100 TiO_2	E_1 0 ZrO_2		563					629		636	
		E_2 .100 ZrO_2				635		605		588		
		E_3 .200 ZrO_2			628		613					665
	D_3 .200 TiO_2	E_1 0 ZrO_2				640		615		593		
		E_2 .100 ZrO_2			617		595					660
		E_3 .200 ZrO_2		616					676		642	

Table 13. ANOVA Young's Modulus of Elasticity

Design Four

Effect	Sum of Squares	Degrees of Freedom	Mean Square	F ratio	Comments
A	47,182.24	2	23,591.12	182.00	Sign. at .01 level
B	5,321.87	2	2,665.94	20.57	Sign. at .01 level
C	46,421.21	2	23,210.61	179.07	Sign. at .01 level
D	9,815.28	2	4,907.64	37.86	Sign. at .01 level
E	12,040.91	2	6,020.46	46.45	Sign. at .01 level
AB	844.06	4	211.02	1.63	Not sign.
AC	1,000.05	4	250.01	1.93	Not sign.
AD	722.88	4	180.72	1.39	Not sign.
AE	399.25	4	99.81	0.77	Not sign.
BC	455.32	4	133.83	0.88	Not sign.
BD	1,311.02	4	327.76	2.53	Sign. at .10 level
BE	536.06	4	134.02	1.03	Not sign.
CD	1,012.35	4	253.09	1.95	Not sign.
CE	3,256.05	4	814.01	6.28	Sign. at .01 level
DE	907.54	4	226.89	1.75	Not sign.
Residual	3,888.64	30	129.62	---	---
Total	135,115.73	80	---	---	---

All five ingredient additions caused increases in Young's modulus. The largest increases were caused by boron and alumina. Silica, zirconia, and titania were responsible for somewhat smaller increases in the modulus. The significant interactions were the alumina-zirconia, and the titania-silica. The titania-silica interaction was that with no titania, increasing silica tends to raise the modulus, while at the two higher levels, silica seems to have very little effect. For the interaction of alumina-zirconia, at both lower levels of zirconia, alumina additions increased Young's modulus. At the highest level of zirconia, the first addition of alumina leaves the modulus unchanged, but the subsequent addition increases Young's modulus considerably.

The multiple regression equations developed for this region of composition form Table 14.

Model equation two was chosen as representing the best fit to the data. Both model equations containing the silica-titania interaction term gave no improvement in the fit. Both the linear and the alumina-zirconia interactional model are satisfactory with model two being given the preference due to its lower standard error of estimate. All four models chosen gave reasonably good fits to the data. The error in using these equations is only very slightly greater than the experimental error. The largest deviation between calculated values using model two and experimentally obtained values for any set of ingredient additions was less than eight per cent.

Table 14. Equations for Young's Modulus

Design Four

Composition Limits

1.0 PbO	0 - 0.250 B_2O_3	1.0 - 2.0 SiO_2
	0 - 0.200 Al_2O_3	0 - 0.200 TiO_2
		0 - 0.200 ZrO_2

X_1 = equiv. B_2O_3 X_2 = equiv. SiO_2

X_3 = equiv. Al_2O_3 X_4 = equiv. TiO_2

X_5 = equiv. ZrO_2

1. Model: Linear

$$E = A_o \pm A_1X_1 \pm A_2X_2 \pm A_3X_3 \pm A_4X_4 \pm A_5X_5$$

$$E = 476 + 236\ X_1 + 18\ X_2 + 295\ X_3 + 107\ X_4 + 126\ X_5$$

Std. error est. = 16.1 Kilobars

2. Model: Alumina-Zirconia Interaction (Best Fit)

$$E = A_o \pm A_1X_1 \pm A_2X_2 \pm A_3X_3 \pm A_4X_4 \pm A_5X_5 \pm A_6/X_3X_5$$

$$E = 468 + 236\ X_1 + 18\ X_2 + 308\ X_3 + 101\ X_4 + 126\ X_5 + 94\ X_3X_5$$

Std. error est. = 13.7 Kilobars

3. Model: Silica-Titania Interaction

$$E = A_o \pm A_1X_1 \pm A_2X_2 \pm A_3X_3 \pm A_4X_4 \pm A_5X_5 \pm A_6/X_2X_4$$

$$E = 474 + 236\ X_1 + 17\ X_2 + 295\ X_3 + 125\ X_4 + 126\ X_5 + 3\ X_2X_4$$

Std. error est. = 16.2 Kilobars

4. Model: Silica-Titania and Alumina-Zirconia Interaction

$$E = A_o \pm A_1X_1 \pm A_2X_2 \pm A_3X_3 \pm A_4X_4 \pm A_5X_5 \pm A_6/X_3X_5 \pm A_7/X_2X_4$$

$$E = 466 + 236\ X_1 + 17\ X_2 + 308\ X_3 + 122\ X_4 + 126\ X_5 + 95\ X_3X_5 + 4\ X_2X_4$$

Std. error est. = 14.8 Kilobars

CHAPTER VI

CONCLUSIONS

1. Red lead is a desirable source of lead in small amounts to prevent reduction of lead glasses.

2. The zirconium compound most easily fusable in a ceramic melt is lead zirconium silicate.

3. Aluminum hydrate is somewhat easier to melt than aluminum oxide. Alumina makes the batch only slightly more refractory.

4. Induction heating is an easier and somewhat more reliable method of smelting experimental glass compositions.

5. Silica additions to a high lead glass increase the melting temperature and viscosity of the melt.

6. Boron reduces the viscosity and lowers melting temperature slightly. Furthermore, it is a valuable aid in dissolving lead zirconium silicate.

7. Zirconia materially increases the melting temperature of the batch and also its viscosity.

8. Titania additions do not significantly change the melting properties of the glass, but have a tendency to turn high lead glasses brownish in color.

9. By obtaining cumulative expansion and temperature data and using the statistical procedure of linear regression, a fairly rapid and accurate method of determining the coefficient of expansion is obtained. This is not the ASTM procedure, but is considerably faster and as accurate.

10. The use of factorial designs in investigating ceramic systems is highly desirable, as interactions between the ingredient additions do occur, and a factorial design is the only means available of discovering these effects.

11. In the region:

1 PbO 0 - 0.375 B_2O_3 1.0 - 2.0 SiO_2

the additions of silica from the lowest level decrease thermal expansion, while the addition of boron has either no effect or a lowering effect, depending on the level of silica content. The best fit equation for the linear coefficient of thermal expansion in this region is:

$$\alpha = 13.48 \times 10^{-6} - 2.10 \times 10^{-6} X_1 - 2.92 \times 10^{-6} X_2 + 6.36 \times 10^{-7} X_1 X_2$$

where: X_1 = equiv. B_2O_3 X_2 = equiv. of SiO_2

The standard error of this estimated equation over this region of compositions is 2.33×10^{-7} in./in./°C.

12. Use of fractional replications for systems containing a large number of variables is a worthwhile technique. Most of the variation in the properties studied were contained in the main effects and the two factor interactions. Thus, a 1/3 replicate of a 3^5 design involving only 1/3 the normal work was an extremely good choice of design for this work.

13. In the region of composition:

1 PbO	0 - 0.250 B_2O_3	1.0 - 2.0 SiO_2
	0 - 0.200 Al_2O_3	0 - 0.200 TiO_2
		0 - 0.200 ZrO_2

alumina, zirconia, and silica all produced significant decreases in the coefficient of thermal expansion. Titania and boron additions did not produce significant changes in the expansion coefficient. Significant in this case means greater than 0.29×10^{-6} in./in./°C. per 0.100 equivalent. The significant interactions were silica-zirconia, and silica-alumina. These were, in both cases, a diminishing of the effectiveness of zirconia and/or alumina with increasing silica content, and a diminishing in the effect of silica at the higher zirconia and alumina contents. In ranked order, zirconia was the most effective in reducing thermal expansion, followed quite closely by silica, and to a somewhat lesser extent followed by alumina. The equation that best fits the data for thermal expansion in this region was:

$$\alpha = 11.89 \times 10^{-6} + 0.55 \times 10^{-6} X_1 - 1.80 \times 10^{-6} X_2 - 4.75 \times 10^{-6} X_3 + 0.24 \times 10^{-6} X_4 - 7.77 \times 10^{-6} X_5 - 0.03 \times 10^{-6}/X_2X_3 - 0.03 \times 10^{-6}/X_2X_5$$

where: X_1 = equiv. of B_2O_3 X_2 = equiv. of SiO_2

X_3 = equiv. of Al_2O_3 X_4 = equiv. of TiO_2

X_5 = equiv. of ZrO_2

The standard error of estimate of this equation was 3.80×10^{-7} in./in./°C.

14. In general, all the glass compositions tested had a relatively low Young's modulus compared to most common glasses. This would make these glasses less brittle, and therefore, more craze resistant. The weaker bond strengths associated with the lower values of Young's modulus

accounts for the low scratch resistance of high lead glazes as compared to lead free glazes.

15. In the region of composition:

1 PbO 0 - 0.375 B_2O_3 1.0 - 2.0 SiO_2

the effects of boron and silica are quite variable in their effect on Young's modulus. The effect of increasing the concentration of one ingredient is dependent upon the level of the other to a large extent. However, in general, both silica and boron additions to lead silicate cause an increase in Young's modulus. The best fit regression equation for Young's modulus in this region was:

$$E = 186 + 244\ X_1 + 346\ X_2 - 106\ X_2^2$$

where:

X_1 = equivalents of boron X_2 = equivalents of silica

The standard error of this estimate is 22.1 Kilobars.

16. It is somewhat significant that for both properties studied, abnormalities occurred at silica level B_2, 1.5 equivalents of silica. The other two levels of silica concentration are both eutectic mixtures of lead and silica, while level B_2 is not. This probably indicates a somewhat regular structure between lead and silica at the non-eutectic compositions and the distribution of the boron more regularly throughout the structural voids. This is indicated by the steady thermal expansion with increasing boron content and the steep rise in Young's modulus.

17. In the composition region:

1 PbO	0 - 0.250 B_2O_3	1.0 - 2.0 SiO_2
	0 - 0.200 Al_2O_3	0 - 0.200 TiO_2
		0 - 0.200 ZrO_2

all ingredient additions in general caused an increase in Young's modulus. The standard error in using the 1/3 replicate of the 3^5 design was not greater than 2.5 per cent. Largest increases in Young's modulus were caused by boron and alumina. Silica, zirconia, and titania were responsible for somewhat smaller increases. The best fit regression equations for this region of composition was:

$$E = 468 + 236\ X_1 + 182\ X_2 + 308\ X_3 + 101\ X_4 + 126\ X_5 + 94\ X_3X_5$$

where: X_1 = equiv. B_2O_3 X_2 = equiv. SiO_2

X_3 = equiv. Al_2O_3 X_4 = equiv. TiO_2

X_5 = equiv. of ZrO_2

APPENDIX A

Table 15. Batch Compositions*

Comp. No.	Pb_3O_4	Lead Monosilicate	H_3BO_3	$Al(OH)_3$	SiO_2	Lead Zirconium Silicate	TiO_2
1	29.1	337.0	---	---	33.8	---	---
2	26.4	304.4	---	---	68.8		
3	24.0	278.0	---	---	98	---	---
4	27.4	319.0	21.1	---	32.0	---	---
5	26.0	304.0	39.2	---	30.4	---	---
6	24.8	290.8	18.8	---	65.6	---	---
7	24.0	276.8	36.0	---	62.8	---	---
8	22.8	266.4	17.2	---	93.2	---	---
9	22.0	256.0	32.8	---	89.6	---	---
10	24.9	290.0	56.4	---	29.2	---	---
11	22.8	265.5	51.7	---	59.9	---	---
12	20.6	239.3	46.5	---	96.0	---	---
13	31.8	240.5	37.3	---	28.2	62.2	---
14	30.2	227.0	17.6	---	66.9	58.8	---
15	28.9	218.0	---	---	96.8	56.3	---
16	32.2	194.6	18.8	---	29.1	125.4	---
17	30.8	186.1	---	---	62.6	120.0	---
18	26.5	160.4	31.0	---	84.0	103.5	---

*Equivalent values are given in Tables 2 and 3.

Table 15. (Continued)

Comp. No.	Pb_3O_4	Lead Monosilicate	H_3BO_3	$Al(OH)_3$	SiO_2	Lead Zirconium Silicate	TiO_2
19	32.2	290.8	37.4	---	29.2	---	9.9
20	30.9	279.0	18.1	---	62.9	---	9.4
21	29.7	267.4	---	---	93.9	---	9.0
22	32.6	245.3	19.4	---	28.8	63.6	9.9
23	31.3	235.6	---	---	63.1	60.9	9.5
24	26.6	199.9	31.0	---	83.4	51.8	8.1
25	33.0	199.8	---	---	29.8	128.2	10.2
26	27.8	168.0	32.8	---	56.3	107.8	8.4
27	26.5	160.4	15.8	---	84.0	103.5	8.0
28	33.1	297.6	19.3	---	29.8	---	20.2
29	31.7	284.6	---	---	64.2	---	19.3
30	26.6	239.3	31.5	---	84.0	---	16.2
31	33.6	252.0	---	---	29.4	65.2	20.3
32	28.1	211.5	33.3	---	56.4	54.8	16.9
33	27.1	203.5	16.0	---	85.0	52.6	16.3
34	29.4	177.5	34.8	---	26.5	114.4	17.7
35	28.2	170.7	16.7	---	57.4	110.1	17.0
36	27.2	164.5	---	---	86.1	106.0	16.4
37	31.6	284.0	37.4	19.2	28.5	---	---
38	30.3	271.5	17.9	18.4	61.4	---	---

Table 15. (Continued)

Comp. No.	Pb_3O_4	Lead Monosilicate	H_3BO_3	$Al(OH)_3$	SiO_2	Lead Zirconium Silicate	TiO_2
39	28.9	260.5	---	17.4	91.5	---	---
40	31.9	239.8	18.9	19.0	28.8	62.1	---
41	30.6	229.8	---	18.2	62.3	59.7	---
42	26.6	199.9	31.5	15.8	84.0	51.8	---
43	32.2	195.0	---	19.2	28.4	125.6	---
44	27.2	164.0	32.2	16.2	54.7	105.8	---
45	26.6	160.4	15.8	15.8	83.4	103.5	---
46	32.2	290.3	19.1	19.6	29.2	---	9.7
47	30.9	278.3	---	18.4	62.9	---	9.3
48	26.6	239.3	31.5	15.8	84.0	---	8.0
49	32.7	246.0	---	19.5	29.5	63.8	9.9
50	27.4	206.5	32.5	16.3	55.8	53.3	8.3
51	26.5	199.9	15.7	15.8	84.0	51.7	8.0
52	28.8	170.5	34.2	17.1	25.8	112.1	8.7
53	27.7	168.0	16.4	16.5	55.9	108.0	8.4
54	26.8	160.4	---	15.8	83.4	103.5	8.0
55	33.1	296.5	---	19.7	29.8	---	20.0
56	27.8	250.2	32.9	16.5	56.5	---	16.8
57	26.6	239.3	15.8	15.8	84.0	---	16.0

Table 15. (Continued)

Comp. No.	Pb_3O_4	Lead Monosilicate	H_3BO_3	$Al(OH)_3$	SiO_2	Lead Zirconium Silicate	TiO_2
58	29.1	218.0	34.4	17.3	26.2	56.6	17.5
59	28.0	210.5	16.6	16.7	56.9	54.6	16.9
60	26.6	199.9	---	15.8	84.0	51.8	16.0
61	29.4	177.8	17.4	17.5	25.9	114.4	17.7
62	28.3	171.0	---	16.8	57.0	110.0	17.1
63	24.3	146.6	28.8	14.4	76.3	94.7	14.6
64	31.5	284.4	18.6	37.5	28.5	---	---
65	30.3	271.5	---	35.9	61.3	---	---
66	25.8	232.0	30.5	30.6	81.6	---	---
67	31.9	239.8	---	37.9	28.8	62.1	---
68	26.9	202.0	31.9	32.0	54.8	52.3	---
69	26.6	199.9	15.8	31.6	84.0	51.8	---
70	28.2	170.5	33.4	33.5	24.8	109.5	---
71	26.5	160.4	15.8	31.6	53.4	103.5	---
72	26.5	160.4	---	31.6	83.4	103.5	---
73	32.4	291.0	---	38.5	29.3	---	9.8
74	27.1	244.5	32.2	32.3	55.1	---	8.2
75	26.6	239.3	15.8	31.6	84.0	---	8.0
76	27.4	214.3	33.7	33.8	25.7	55.2	8.6
77	27.3	205.0	18.0	32.5	55.6	53.1	8.2

Table 15 (Continued)

Comp. No.	Pb_3O_4	Lead Mono-silicate	H_3BO_3	$Al(OH)_3$	SiO_2	Lead Zirconium Silicate	TiO_2
78	26.6	199.9	---	31.6	84.0	51.8	8.0
79	28.8	173.7	17.1	34.2	25.3	112.2	8.7
80	27.7	167.3	---	33.0	55.7	108.0	8.4
81	23.4	141.8	27.8	27.9	73.8	91.5	14.9
82	28.8	259.2	34.1	34.2	26.0	---	17.4
83	27.7	250.0	16.4	32.9	56.3	---	16.7
84	26.6	239.3	---	31.6	84.0	---	16.0
85	29.1	218.5	17.3	34.6	26.3	56.6	17.5
86	28.1	211.0	---	33.4	57.1	54.1	16.9
87	24.2	181.5	29.5	29.6	76.3	46.8	14.6
88	29.4	177.4	---	35.0	25.9	114.6	17.7
89	25.2	152.9	28.6	28.7	59.5	86.6	15.1
90	24.3	146.7	14.4	28.9	76.3	94.8	14.7

APPENDIX B

LINEAR REGRESSION

The linear regression procedure is a method of obtaining a least squares fit to data that show a linear trend. As an example of this calculation, the data for composition 70 will be used. The procedure is applied to all values obtained up to the transformation temperature of the glass. Data collected for this specimen comprises Table 16. Graphical treatment of the data is Figure 7. The transformation temperature is 484°C., while the softening temperature of the specimen is 595°C.

The slope of the regression line is b, where:

$$b = \frac{\Sigma XY - \bar{X}\Sigma Y}{\Sigma X^2 - n\bar{X}^2} \qquad (10)$$

The Y intercept is a, where:

$$a = \bar{Y} - b\bar{X} \qquad (11)$$

Thus, the equation for the straight line has the familiar form:

$$Y = a + bX \qquad (12)$$

The calculations of the necessary values are easily handled on a desk calculator. By using the left hand side of the calculator for temperature, i.e. "X", and the right side for cumulative expansion, i.e. "Y", the value of ΣY, ΣY, ΣX^2, ΣY^2, and $2\Sigma XY$ can be found by one pass through the machine. Calculated values are seen in Table 17.

Table 16. Expansion Data Composition 70

Length of Specimen 2.330 in.			
Time	Amperage	X Temperature	Y Cumulative Expansion x 10^3
11:22	3.5	20	0.00
11:30	3.5	44	0.07
11:35	3.5	70	0.29
11:40	3.5	100	0.61
11:45	3.5	129	0.98
11:50	3.5	155	1.39
11:55	3.8	182	1.77
12:00	3.8	210	2.19
12:05	4.0	235	2.58
12:10	4.2	262	2.99
12:15	4.4	291	3.41
12:20	4.4	317	3.79
12:25	4.6	345	4.21
12:30	4.6	374	4.61
12:35	4.6	401	5.02
12:40	4.8	426	5.41
12:45	5.0	455	5.82
*12:50	5.0	484	6.28
12:55	5.0	511	6.82
1:00	5.0	532	7.68
1:05	5.4	557	9.08
1:10	5.4	580	9.98
** 1:15	5.4	595	9.98

*Transformation Temp.

**Softening Temp.

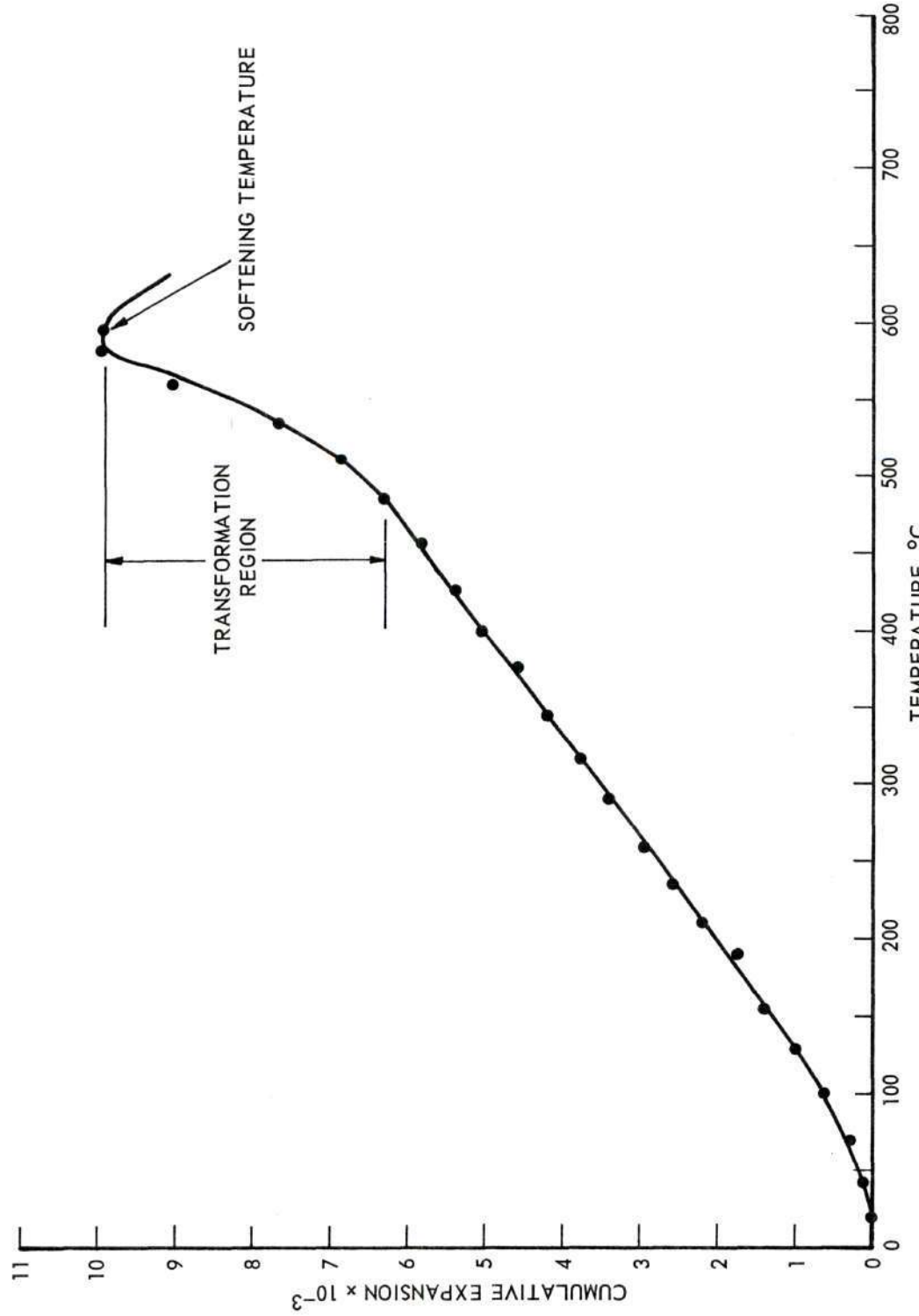

Figure 7. Thermal Expansion Composition 70.

Table 17

Calculation of the Regression Equation

ΣX	= 4500	n	= 18
ΣY	= 51.42	$\bar{X}$	= 250.00
ΣX^2	= 1,486,624	ΣXY	= 17,973.60
$2\Sigma XY$	= 35,947.20	$\bar{X}\Sigma Y$	= 12,855.00
ΣY^2	= 219.6268	$\bar{X}^2$	= 62,500.00
		$n\bar{X}^2$	= 1,125,000.00

$$b = \frac{\Sigma XY - \bar{X}\Sigma Y}{\Sigma X^2 - n\bar{X}^2} = \frac{5118.60}{361,624.00} = 14.15448 \times 10^{-6}$$

$$a = \bar{Y} - b\bar{X}$$

$$a = 2.86 \times 10^{-3} - 3.54 \times 10^{-3} = -0.68 \times 10^{-3}$$

$$Y = 14.15 \times 10^{-6} X - 0.68 \times 10^{-3}$$

The linear coefficient of thermal expansion is found by the equation:

$$\alpha = \frac{b}{\text{Length of specimen}} + 0.54 \times 10^{-6*} \qquad (13)$$

Thus the coefficient of thermal expansion will equal:

$$\alpha = \frac{14.15448}{2.330} \times 10^{-6} + 0.54 \times 10^{-6}$$

$$\alpha = 6.61 \times 10^{-6}$$

*Correction factor for fused silica expansion in dialatometer furnace.

APPENDIX C

ANALYSIS OF DESIGN ONE

The data collected for Design One appears as Table 3 in the discussion of results. Table 18 shows a worksheet format for the calculation of the analysis of variance, Table 4.

Table 18. Analysis of Variance Workshop

Effect	Sum of Squares	Degrees of Freedom	Mean Square
Boron	$C_A - C$	$a - 1$	$\frac{C_A - C}{a - 1}$
Silica	$C_B - C$	$b - 1$	$\frac{C_B - C}{b - 1}$
Boron and Silica Int.	$C_{AB} - C_A - C_B + C$	$(a - 1)(b - 1)$	$\frac{C_{AB} - C_A - C_B + C}{(a - 1)(b - 1)}$
Experimental Error	$C_{R(AB)} - C_{AB}$	$r(a - 1)(b - 1)$	$\frac{C_{R(AB)} - C_{AB}}{r(a - 1)(b - 1)}$
Total	$C_{R(AB)} - C$	$abr - 1$	----

In the first column on the left, the possible effects in this experiment are listed. First, boron and silica are the two main effects. Next comes the boron silica interaction. The experimental error is "broken away" from the other effects. The manner in which the procedure works is: if the deviations coming from the particular effect of interest

are statistically greater than the experimental error, then numbers this large could not possibly have come from the experimental error. Therefore, the effect under consideration must be of real significance in determining the coefficient of thermal expansion in this case.

The second column is entitled the sum of squares. The letters in this column are a shorthand notation. For example, for the main effect, boron, C_A is equal to the sum of the squares of the data summed over everything except the four levels of the boron content divided by six, the number of observations summed over. The letter C stands for the correction factor due to the mean, which is equal to the grand total of the trials squared divided by 24, the total number of trials in this experiment.

In a similar manner, the other sums of squares are found, in each case summing over everything but the factor of interest, and squaring and dividing by the number of trials summed over. Finally, the total sum of squares is calculated independently and this value is compared to the total of all the other sums of squares to provide a check on mathematical computations.

The third column is labeled degrees of freedom. For simplicity, this is equal to one less than the number of levels of the factor under consideration. For example, boron with four levels has three degrees of freedom. For interaction terms, the degrees of freedom are equal to the product of the degrees of freedom terms making up the interaction. For the experimental error effect, the term r, which stands for replications, is equal to two. One is not subtracted, as this is what is called a nested factor. The total degrees of freedom for the whole experiment are equal

to the total number of trials minue one.

The symbolism for the calculation of the mean squares is in the last column. It may be observed that this is simply equal to the quotient of the sum of squares divided by the degrees of freedom.

Table 19 gives the complete analysis of variance for this design. The values in the first four columns were obtained in the manner just described. Column number five, entitled F ratio, is the quotient of the mean square of the particular effect divided by the experimental error mean square. If the F ratio obtained is statistically greater than one, then the effect under consideration is a contributing factor to the observed coefficient of expansion. How much greater than one does the F ratio have to be to say that the effect is real? The answer to this question can be found in a compilation of the F distribution found in many of the common handbooks (29) and all statistical texts (19). It turns out that the interaction term is significant, and the silica term, because of its extremely high F ratio, is significant. The boron effect is only possibly significant, due to the fact that there is an interaction present in this experiment.

In the last column of this table, entitled the expected mean square, the reasoning behind the F ratio test may be observed. The experimental error is made up of one term, sigma sub zero, while the interaction term is composed of two terms, sigma sub zero plus another term expressing the average magnitude of the interaction. If this second term is zero, then the F ratio obtained would be statistically equal to one. It is an F ratio since it represents the quotient of mean square terms. If the second term is not zero, then the ratio would be

Table 19. Analysis of Variance Design One

Effect	Sum of Squares	Degrees of Freedom	Mean Square	F Ratio	Expected Mean Square
Boron	0.7594	3	0.2531	9.20	$\sigma_o^2 + rs\sigma_B^2$
Silica	32.1497	2	16.0739	584.51	$\sigma_o^2 + rb\sigma_S^2$
Boron and Silica Int.	0.6487	6	0.1081	3.93	$\sigma_o^2 + r\sigma_{BS}^2$
Experimental Error	0.3294	12	0.0275	----	σ_o^2
Total	33.8872	23	----	----	----

statistically greater than one, and an interaction would exist. Since the two main effects have two terms making up their respective expected mean square terms these may also be tested against the experimental mean square. However, since the interaction in this experiment is significant no real significance can be placed on this test as the interaction must first be investigated.

Figure 8 is a graphical treatment of the average values of the coefficient of thermal expansion found. At level B_1, 1.0 equivalents of silica, there is at first a lowering and then a leveling off of the coefficient of thermal expansion with increasing boron content. Also at level B_3, 2.0 equivalents of silica, if point two is ignored, a sharp drop is seen and then a leveling off. It is entirely possible that point two could be below point one, as experimental error may account

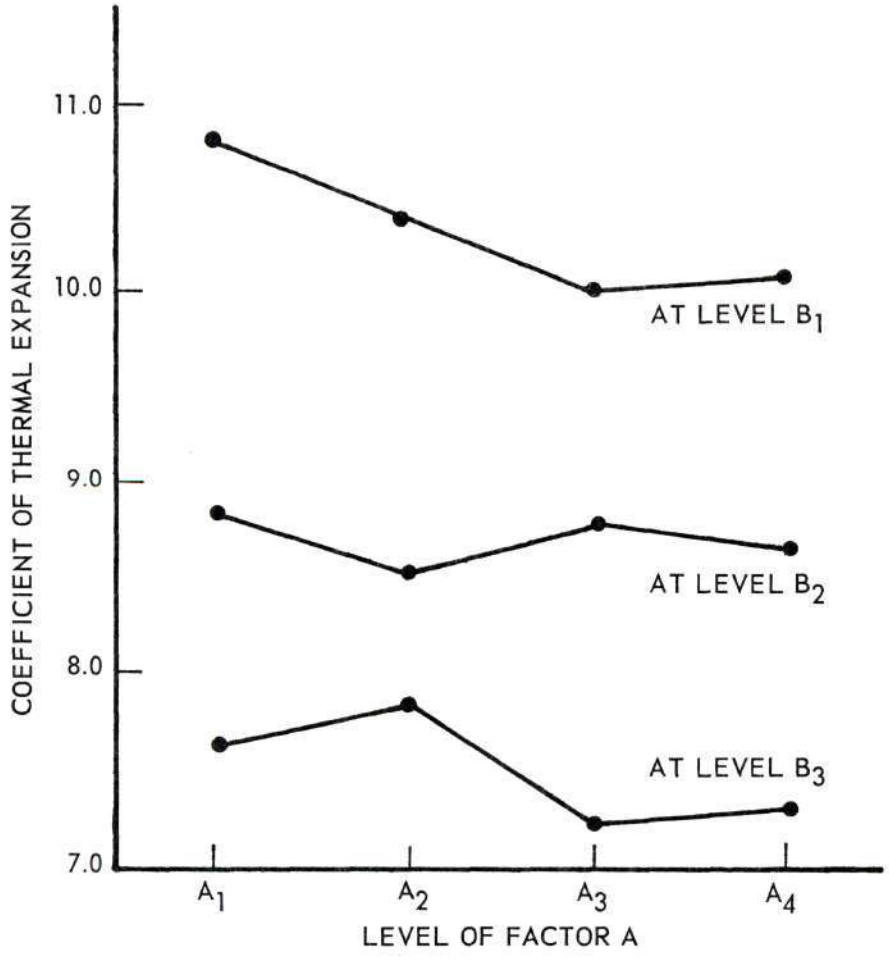

Figure 8. Average Values of Coefficient of Expansion x 10^6 in./in./°C.

for its high position. However, at level B_2, no sharp drop off of coefficient of expansion is noted with increasing boron content. The up and down movements of the values obtained could be due to experimental error, and in reality this could be a straight line. Therefore, the interaction in this experiment is, in all probability, the lowering of the coefficient of thermal expansion by boron at levels B_1 and B_3, but not at level B_2.

A statistical verification of these observations can be found by use of Duncan's Multiple Range Test, Table 20. The standard error of the mean is equal to the square root of the mean square of the experimental error, sigma sub-zero, divided by the number of trials in the average. In this case, there are two trials in the average, representing the two replications of the experiment. In the first column of this table, p is the number of values in the range. The second column, entitled significant range, contains the values obtained from a table of Duncan's Multiple Range Test. The third column, least significant range is the product of the standard error of the mean multiplied by the significant range. At level B_1, the coefficient of expansion at level A_1, no boron, is significantly greater than at the higher boron contents. Thus the boron additions to a composition of one equivalent of lead oxide and one equivalent of silica decreased the thermal expansion. Also, there is a leveling off of this decrease in expansion as the boron is increased. The same sort of thing holds true at level B_3, 2.0 equivalents of silica. It will also be noted that levels A_1 and A_2 of the boron content do not give a significantly different value, and therefore the rise in the coefficient of thermal expansion noted between these two levels could have been due

Table 20. Duncan's Multiple Range Test

Standard Error of Mean = $S_{\bar{x}} = \sqrt{\frac{0.0275}{2}} = 0.1173$

p	Significant Range One Per Cent Level	Least Significant Range One Per Cent Level
2	4.32	0.51
3	4.55	0.53
4	4.68	0.55

at Level B_1

Level	A_3	A_4	A_2	A_1
Mean	10.04	10.13	10.41	10.82

at Level B_2

Level	A_2	A_4	A_3	A_1
Mean	8.57	8.68	8.84	8.88

at Level B_3

Level	A_3	A_4	A_1	A_2
Mean	7.22	7.32	7.68	7.86

Note: Lines are drawn under those means which are found to be not significantly different. A difference is significant if it exceeds the corresponding least significant range.

entirely to experimental error, and no significance can be attached to this increase. At level B_2, 1.5 equivalents of silica, none of the values obtained with increasing boron content differs significantly from each

other. Therefore, it cannot be stated that there was any boron effect at the 1.5 equivalent level of the silica content. Thus, this is the interaction detected with the analysis of variance procedure. The effect of boron is different at different levels of the silica content.

The best estimate of the magnitude of the experimental error is 0.1658×10^{-6} in./in./°C. as seen in Table 21. This value represents about 1.8 per cent of the average size of the values obtained for the coefficient of expansion. The upper 90 per cent confidence limit on this value is 0.3512×10^{-6} in./in./°C., and the lower 90 per cent confidence limit is 0.1253×10^{-6} in./in./°C. Thus, with 90 per cent confidence, the true value of the standard deviation due to experimental error lies in the range 0.1253×10^{-6} to 0.2512×10^{-6} in./in./°C.

Table 21. Standard Deviation Due to Experimental Error.

Best Estimate = $S_o = 0.1658 \times 10^{-6}$
Upper 90 per cent Confidence Limit = $\sqrt{\frac{12\, S_o^2}{\chi^2_{0.95;\,12}}} = 0.2512 \times 10^{-6}$
Lower 90 per cent Confidence Limit = $\sqrt{\frac{12\, S_o^2}{\chi^2_{0.05;\,12}}} = 0.1253 \times 10^{-6}$

APPENDIX D

MULTIPLE REGRESSION ANALYSIS PROGRAM

Multiple regression analysis relates the dependent variable, in this case coefficient of thermal expansion or Young's modulus, to the independent variables, i.e. composition variables, by means of a linear equation, and determines how well each equation fits the data. Normal equations are developed with the sums of squares and cross products which are corrected to the mean, and the abbreviated Doolittle method is employed to invert this matrix and to calculate the regression coefficients.

If Y' is used to estimate the dependent variable Y by means of a linear function of the independent variables $X_1,\ldots,X_N$ and $x(i) = X(i) - \bar{X}(i)$, $y' = Y' - \bar{Y}$, $y = Y - \bar{Y}$, then each regression equation is assumed to be of the form:

$$y' = \sum_{i=1}^{N} b(i)\, x(i) \tag{14}$$

where: $b(i)$ = a regression coefficient

$x(i)$ = an independent variable corrected for the mean

$X(i)$ = an independent variable

The error in estimating a single value Y will be:

$$Y - Y' = y - y' = y - \sum_{i=1}^{N} b(i)\, x(i) \tag{15}$$

The least squares method determines values $b(i)$ so that the sum of squares:

$$\sum \left[y - \sum_{i=1}^{N} b(i)\ x(i) \right]^2 \tag{16}$$

is a minimum. Partial differentiation produces a set of normal equations whose coefficients are $\Sigma\Sigma\ X(i)\ x(j)$ and whose constant terms are $\Sigma\Sigma\ x(i)y$; $j = 1,\ldots,N$. The abbreviated Doolittle method is employed to solve these equations for $b(i)$. After the inverse coefficient matrix $(C(ij))$ is obtained, the regression coefficients are calculated by:

$$b(i) = C(i1)\ \Sigma\ x(1)y + \ldots + C(iN)\ \Sigma\ x(N)y \tag{17}$$

The final equation has the form

$$a = b_o + b_1 x_1 + b_2 x_2 + \ldots + b_n x_n + E \tag{18}$$

where $b_o, b_1,\ldots,b_n$ are the regression coefficients and E is the experimental error. The standard error of the estimate is

$$S = \sqrt{\frac{\Sigma(y - y')^2}{M - N - 1}} \tag{19}$$

The program (11) will give a least squares fit to any model equation by a switch command to any combination of functions in any order.

APPENDIX E

ANALYSIS OF DESIGN TWO

The analysis of design two by the analysis of variance procedure is handled by a series of two factor tables. These tables are formed by summing over everything but the two factors of interest. From them all the main effects and two factor interactions may be calculated. The two way tables and their sums of squares are Tables 22 through 31. The total sum of squares for the data is obtained by squaring all 81 observations and adding then subtracting the correction factor, C. By summing the sums of squares of the main effects and two factor interactions, and subtracting this from the total sum of squares, the residual factor is obtained. The degrees of freedom are calculated in the usual manner for the two factor interactions and main effects. There are 80 degrees of freedom for the whole experiment, 50 are taken up by the main effects and two factor interactions and the residual term has the remaining 30 degrees of freedom. The test procedure in this case is to divide the residual mean square into the particular effect mean square, obtaining an F ratio. This value is compared to a value from the F distribution with the indicated degrees of freedom to assess the statistical significance of the effect. The complete ANOVA table was Table 7.

It is significant to point out that the trends found in Design One hold in Design Two, namely that the effect of boron is different at level B_2 of the silica content, as seen in Table 22. As has been

mentioned previously, the significant interactions in this experiment are the alumina-silica, and the zirconia-silica interactions. The interaction in both cases seems to be a diminishing effect of the power of these ingredients in lowering the thermal expansion when the other is at its highest level. Graphical treatment of the data is seen in Figures 9 and 10. Duncan's Multiple Range Test is also included for these curves as seen in Table 32. Table 33 gives the best estimate of the magnitude of the residual interactions plus experimental error.

From Tables 22 - 31 it seems as though there are many violations of trends. However, only two significant interactions were found. The other small violations in trends could be due entirely to experimental error or high order interactions. The magnitude of this factor is 0.2901×10^{-6} in./in./°C. which could account for errors as large as 3.8 per cent in the data.

Table 22. Data Summed Over Factors CDE

Level of Factor A

Equivalents of Boron

Level of Factor B Equivalents of Silica	A_1 0 B_2O_3	A_2 0.125 B_2O_3	A_3 0.250 B_2O_3	Total
B_1 1.0 SiO_2	75.54	76.85	77.91	230.30
B_2 1.5 SiO_2	69.29	69.46	68.56	207.31
B_3 2.0 SiO_2	61.67	62.05	63.73	187.45
Total	206.50	208.36	210.20	625.06

$$C = \frac{390,700.0036}{81} = 4,823.45683$$

$$C_A = \frac{130,240.1796}{27} = 4,823.71035$$

$$C_B = \frac{131,153.0286}{27} = 4,857.51957$$

$$C_{AB} = \frac{43,723.3558}{9}$$

$$SS_A = 0.25352$$

$$SS_B = 34.06274$$

$$SS_{AB} = 0.37755$$

$$SS_{total} = 34.69381$$

Table 23. Data Summed Over Factors BDE

Level of Factor A

Equivalents of Boron

Level of Factor C, Equivalents of Al_2O_3	A_1 0 B_2O_3	A_2 0.125 B_2O_3	A_3 0.250 B_2O_3	Total
C_1 0 Al_2O_3	73.77	74.31	75.26	223.34
C_2 0.100 Al_2O_3	68.15	68.19	69.99	206.33
C_3 0.200 Al_2O_3	64.58	65.86	64.95	195.39
Total	206.50	208.36	210.20	625.06

$C = 4,823.45683$

$C_A = 4,823.71035$

$C_C = 4,838.15098$

$C_{AC} = 4,838.61931$

$SS_A = 0.25352$

$SS_C = 14.69415$

$SS_{AC} = 0.21481$

$SS_{total} = 15.16248$

Table 24. Data Summed Over Factors BCE

Level of Factor A

Equivalents of Boron

Level of Factor D, Equivalents of TiO_2	A_1 0 B_2O_3	A_2 0.125 B_2O_3	A_3 0.250 B_2O_3	Total
D_1 0 TiO_2	68.11	68.84	70.03	206.98
D_2 0.100 TiO_2	68.90	70.40	70.51	209.81
D_3 0.200 TiO_2	69.49	69.12	69.66	208.27
Total	206.50	208.36	210.20	625.06

$C = 4,823.45683$

$C_A = 4,823.71035$

$C_D = 4,823.60553$

$C_{AD} = 3,823.01097$

$SS_A = 0.25352$

$SS_D = 0.14870$

$SS_{AD} = 0.15192$

$SS_{total} = 0.55414$

Table 25. Data Summed Over Factors BCD

Level of Factor A

Equivalents of Boron

Level of Factor E, Equivalents of ZrO_2	A_1 0 B_2O_3	A_2 0.125 B_2O_3	A_3 0.250 B_2O_3	Total
E_1 0 ZrO_2	77.55	77.84	77.92	233.31
E_2 0.100 ZrO_2	66.78	67.83	69.76	204.37
E_3 0.200 ZrO_2	62.17	62.69	62.52	187.38
Total	206.50	208.36	210.20	625.06

$C = 4,823.45683$

$C_A = 4,823.71035$

$C_E = 4,863.40434$

$C_{AE} = 4,863.93608$

$SS_A = 0.25352$

$SS_E = 39.94751$

$SS_{AE} = 0.27822$

$SS_{total} = 30.47925$

Table 26. Data Summed Over Factors ADE

Level of Factor B

Equivalents of SiO_2

Level of Factor C, Equivalents of Al_2O_3	B_1 1.0 SiO_2	B_2 1.5 SiO_2	B_3 2.0 SiO_2	Total
C_1 0 Al_2O_3	84.15	74.52	64.67	223.34
C_2 0.100 Al_2O_3	75.92	68.24	62.17	206.33
C_3 0.200 Al_2O_3	70.23	64.55	60.61	195.39
Total	230.30	207.31	187.45	625.06

$C = 4,823.45683$

$C_B = 4,857.51957$

$C_C = 4,838.15098$

$C_{BC} = 4,874.98246$

$SS_B = 34.06274$

$SS_C = 14.69415$

$SS_{BC} = 2.76874$

$SS_{total} = 51.52563$

Table 27. Data Summed Over Factors ACE

Level of Factor B

Equivalents of SiO_2

Level of Factor D
Equivalents of TiO_2

	B_1 1.0 SiO_2	B_2 1.5 SiO_2	B_3 2.0 SiO_2	Total
D_1 0 TiO_2	77.64	68.34	61.60	206.98
D_2 0.100 TiO_2	76.72	69.29	63.80	209.81
D_3 0.200 TiO_2	76.54	69.68	62.05	208.27
Total	230.30	207.31	187.45	625.06

$C = 4,823.45683$ $SS_B = 34.06274$

$C = 4,857.51957$ $SS_D = 0.14870$

$C_D = 4,823.60553$ $SS_{BD} = 0.27130$

$C_{BD} = 4,857.93957$ $SS_{total} = 34.48274$

Table 28. Data Summed Over Factors ACD

Level of Factor B

Equivalents of SiO_2

Level of Factor E, Equivalents of ZrO_2	B_1 1.0 SiO_2	B_2 1.5 SiO_2	B_3 2.0 SiO_2	Total
E_1 0 ZrO_2	88.14	76.57	68.60	233.31
E_2 0.100 ZrO_2	75.17	67.66	61.54	204.37
E_3 0.200 ZrO_2	66.99	63.08	57.31	187.38
Total	230.30	207.31	187.45	625.06

$C = 4,823.45683$

$C_B = 4,857.51957$

$C_E = 4,863.40434$

$C_{BE} = 4,900.48257$

$SS_B = 34,06274$

$SS_E = 39.94751$

$SS_{BE} = 3.01549$

$SS_{total} = 77.02574$

Table 29. Data Summed Over Factors ABE

Level of Factor C

Equivalents of Al_2O_3

Level of Factor D, Equivalents of TiO_2	C_1 0 Al_2O_3	C_2 0.100 Al_2O_3	C_3 0.200 Al_2O_3	Total
D_1 0 TiO_2	74.61	68.20	64.17	206.98
D_2 0.100 TiO_2	74.20	68.74	66.87	209.81
D_3 0.200 TiO_2	74.53	69.39	64.35	208.27
Total	223.34	206.33	195.39	625.06

$C = 4,823.45683$

$C_C = 4,838.15098$

$C_D = 4,823.60553$

$C_{CD} = 4,838.74677$

$SS_C = 14.69415$

$SS_D = 0.14870$

$SS_{CD} = 0.44709$

$SS_{total} = 15.28994$

Table 30. Data Summed Over Factors ABD

Level of Factor E (Equivalents of ZrO_2)	Level of Factor C (Equivalents of Al_2O_3)			
	C_1 0 Al_2O_3	C_2 0.100 Al_2O_3	C_3 0.200 Al_2O_3	Total
E_1 0 ZrO_2	82.13	77.57	73.61	233.31
E_2 0.100 ZrO_2	73.91	67.78	62.68	204.37
E_3 0.200 ZrO_2	67.30	60.98	59.10	187.38
Total	223.34	206.33	195.39	625.06

$C = 4,823.45683$

$C_C = 4,838.15098$

$C_E = 4,863.40434$

$C_{CE} = 4,878.57035$

$SS_C = 14.69415$

$SS_E = 39.94751$

$SS_{CE} = 0.47186$

$SS_{total} = 55.11352$

Table 31. Data Summed Over Factors ABC

Level of Factor D

Equivalents of TiO_2

Level of Factor E

Equivalents of ZrO_2

	D_1 0 TiO_2	D_2 0.100 TiO_2	D_3 0.200 SiO_2	Total
E_1 0 ZrO_2	78.24	78.57	76.50	233.31
E_2 0.100 ZrO_2	67.35	68.42	68.60	204.37
E_3 0.200 ZrO_2	61.39	62.82	63.17	187.38
Total	206.98	209.81	208.27	625.06

$C = 4,823.45683$

$C_D = 4,823.60553$

$C_E = 4,863.40434$

$C_{DE} = 4,863.97831$

$SS_D = 0.14870$

$SS_E = 39.94751$

$SS_{DE} = 0.42527$

$SS_{total} = 40.52148$

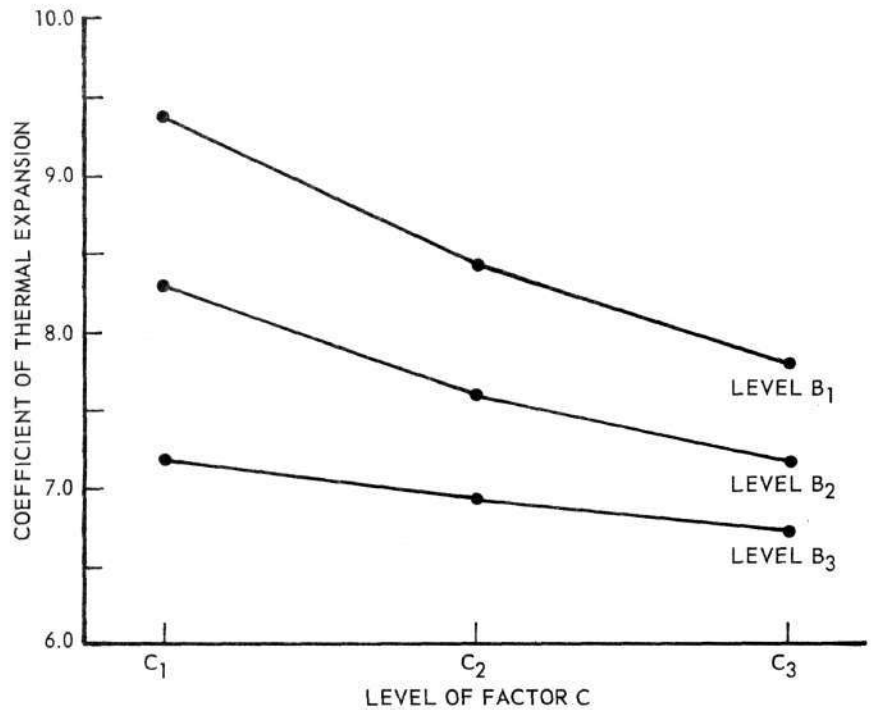

Figure 9. Average Values of Coefficient of Expansion x 10^6 in./in./°C.

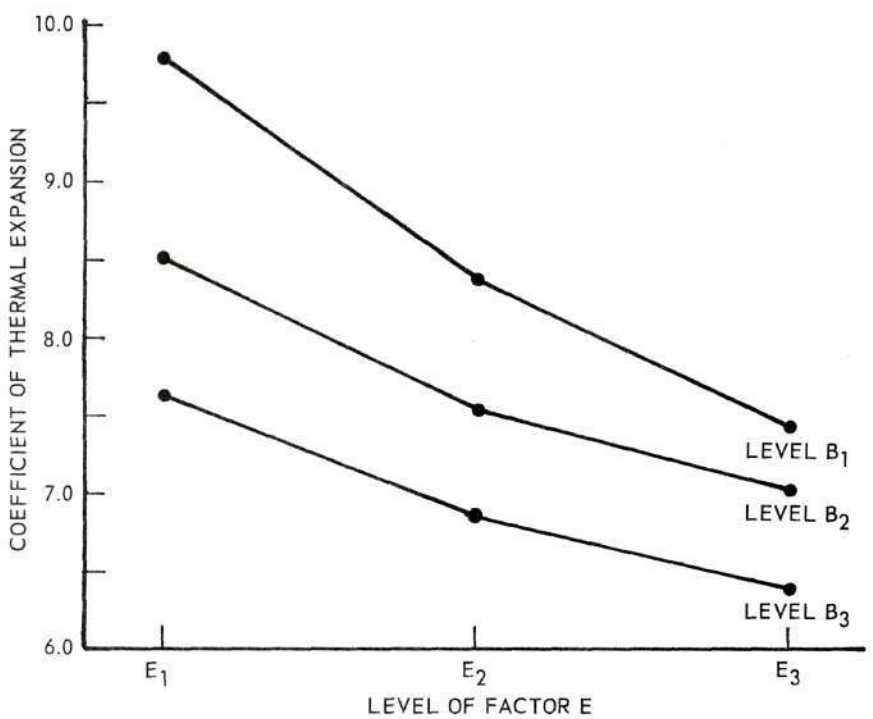

Figure 10. Average Values of Coefficient of Thermal Expansion x 10^6 in./in./°C.

Table 32. Duncan's Multiple Range Test For Interactions Design Two

Standard Error of Mean = $S_{\bar{x}} = \sqrt{\frac{0.08427}{9}} = 0.0967$

p	Significant Range One Per cent Level	Least Significant Range One Per Cent Level
2	3.89	0.38
3	4.06	0.39

For Alumina-Silica Interaction

At Level B_1

Level	C_3	C_2	C_1
Mean	7.80	8.44	9.35

At Level B_2

Level	C_3	C_2	C_1
Mean	7.17	7.58	8.22

At Level B_3

Level	C_3	C_2	C_1
Mean	6.73	6.91	7.19

For Zirconia-Silica Interaction

At Level B_1

Level	E_3	E_2	E_1
Mean	7.44	8.35	9.79

(Continued)

Table 32. (Continued)

At Level B_2			
Level	E_3	E_2	E_1
Mean	7.01	7.52	8.51
At Level B_3			
Level	E_3	E_2	E_1
Mean	6.37	6.84	7.62

Table 33. Best Estimate of the Magnitude of the Residual Interactions Plus Experimental Error Design Two

Best Estimate = $S_o = 0.2901 \times 10^{-6}$ in./in./°C

Upper 90 per cent Confidence Limit = $\sqrt{\frac{30\ So^2}{\chi^2_{0.95;\ 30}}} = 0.3696 \times 10^{-6}$ in./in./°C.

Lower 90 per cent Confidence Limit = $\sqrt{\frac{30\ So^2}{\chi^2_{0.05;\ 30}}} = 0.2403 \times 10^{-6}$ in./in./°C.

APPENDIX F

DETAILS OF DESIGN THREE

Design Three is analyzed in exactly the same manner as Design One, Appendix C. The interaction is again significant. Figure 7 is a graphical treatment of the average values found. It would seem that the pattern on Levels B_1 and B_3 is roughly the same, but for Level B_2, 1.5 equivalents of silica, increasing boron has a somewhat different effect. It also appears that at Level A_4, 0.375 equivalents of boron maximum strength is approached at Levels B_1 and B_3, while at Level B_2 maximum strength is reached at Level A_3, 0.250 equivalents of boron. Thus, it would seem that the glass is strengthened up to a maximum level with boron at a given level of silica and further additions weaken the glass, or possibly leave it unchanged.

Duncan's Multiple Range Test for this design is Table 34. It is easily seen from this test that the effect of boron is different at Level B_2, 1.5 equivalents of silica, than it is at Levels B_1 and B_3, 1.0 and 2.0 equivalents, respectively. Also, Levels A_4B_2, A_4B_1, A_3B_2 do not differ significantly. Thus, from this design it seems as though Young's modulus for this range of compositions approaches a maximum. It is conceivably possible that at higher levels of boron Young's modulus would decrease. However, any more boron in these glasses would render them commercially useless due to their low chemical resistance.

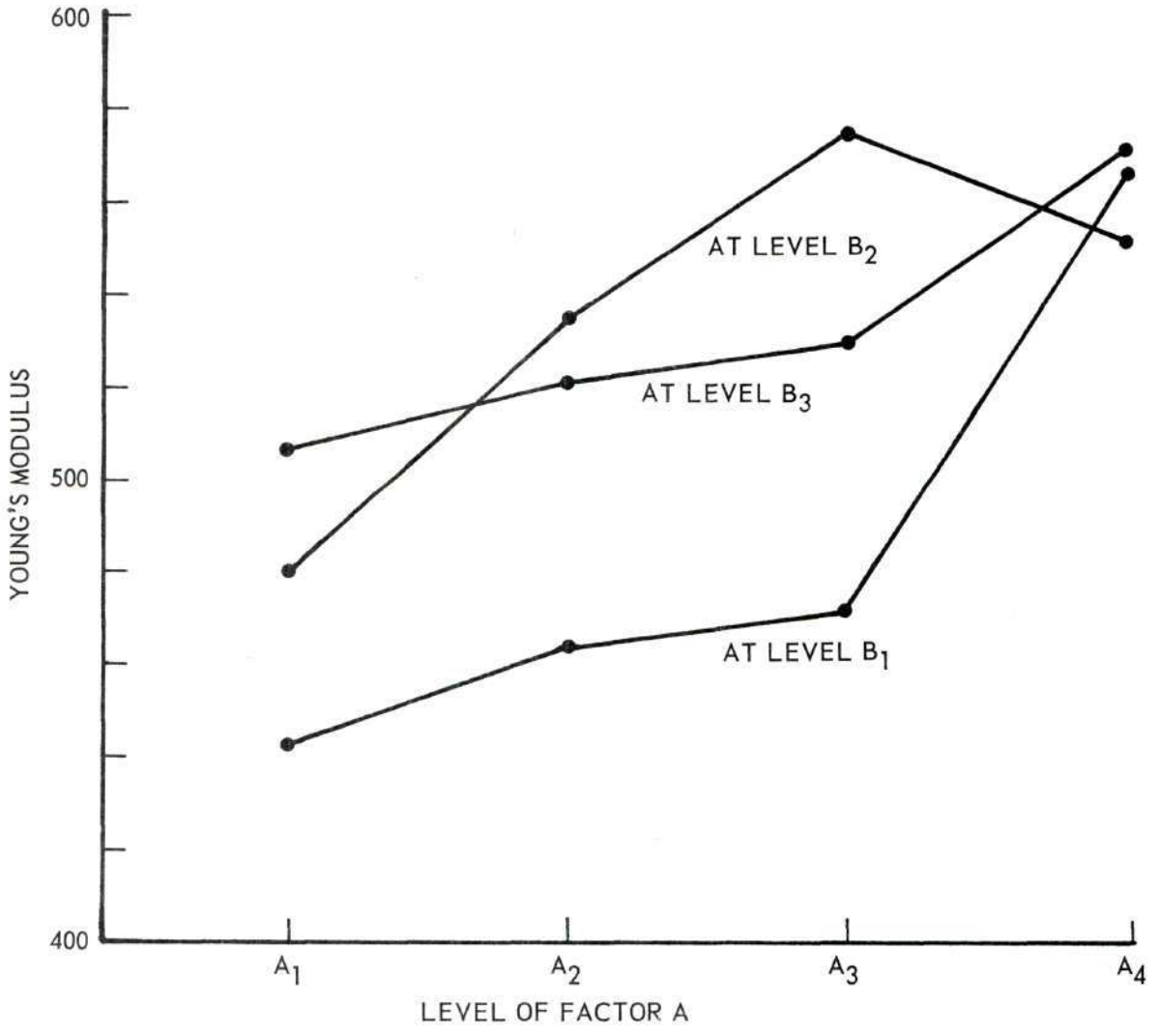

Figure 11. Average Values of Young's Modulus in Kilobars.

Table 34. Duncan's Multiple Range Test
Design Three

Standard Error of Mean = $S_{\bar{x}} = \sqrt{\frac{112.71}{2}} = 7.507$

p	Significant Range One Per Cent Level	Least Significant Range One Per Cent Level
2	4.32	32
3	4.55	34
4	4.68	35

At Level B_1

Level	A_1	A_2	A_3	A_4
Mean	442	463	472	567

At Level B_2

Level	A_1	A_2	A_3	A_4
Mean	480	535	552	575

At Level B_3

Level	A_1	A_2	A_3	A_4
Mean	508	521	529	572

Note: Lines are drawn under those means which are found to be not significantly different. A difference is significant if it exceeds the corresponding least significant range.

Table 35. Standard Deviation Due to Experimental Error in Kilobars Design Three

---

Best Estimate = S_o = 10.62 Kilobars

Upper 90 per cent Confidence Limit = $\sqrt{\frac{12\, S_o^2}{\chi^2_{0.95;\, 12}}}$ = 16.04 Kilobars

Lower 90 per cent Confidence Limit = $\sqrt{\frac{12\, S_o^2}{\chi^2_{0.05;\, 12}}}$ = 8.02 Kilobars

---

Table 35 gives the standard deviation due to experimental error. Also included in this table are the upper and lower confidence levels on this value. This value represents about 2.1 per cent of the size of the values obtained in this experiment.

APPENDIX G

ANALYSIS OF DESIGN FOUR

Design Four is analyzed in the same manner as Design Two, Appendix E. The two way analysis of variance tables and their sums of squares comprise Tables 36 through 45. Completed analysis of variance table appeared as Table 13, in the discussion of results.

The significant interactions are shown in graphical form, Figures 12 and 13. Duncan's Multiple Range Test is Table 46. By use of equations (21) and (22), it is found that the difference between averages must be equal to 16 Kilobars before they can be considered significant, and the differences between cumulative values must be equal to 138 to be significant. Table 47 gives the best estimate of the error in this design, together with the upper and lower 90 per cent confidence limits on this error.

Table 36. Data Summed Over Factors CDE

Level of Factor A

Equivalents of B_2O_3

Level of Factor B, Equivalents of SiO_2	A_1 0 B_2O_3	A_2 0.125 B_2O_3	A_3 0.250 B_2O_3	Total
B_1 1.0 SiO_2	4,855	5,177	5,430	15,462
B_2 1.5 SiO_2	5,039	5,213	5,570	15,822
B_3 2.0 SiO_2	5,083	5,331	5,572	15,986
Total	14,977	15,721	16,572	47,270

$C = 27,585,838.27$

$C_A = 27,633,020.51$

$C_B = 27,591,160.14$

$C_{AB} = 27,639,186.44$

$SS_A = 47,182.24$

$SS_B = 5,321.87$

$SS_{AB} = 844.06$

$SS_{total} = 53,348.17$

Table 37. Data Summed Over Factors BDE

Level of Factor C (Equivalents of Al_2O_3)	Level of Factor A (Equivalents of B_2O_3)			
	A_1 0 B_2O_3	A_2 0.125 B_2O_3	A_3 0.250 B_2O_3	Total
C_1 0 Al_2O_3	4,710	5,005	5,344	15,059
C_2 0.100 Al_2O_3	4,979	5,189	5,426	15,594
C_3 0.200 Al_2O_3	5,288	5,527	5,802	16,617
Total	14,977	15,721	16,572	47,270

$C = 27,585,838.27$

$C_A = 27,633,020.51$

$C_C = 27,632,259.48$

$C_{AC} = 27,680,441.77$

$SS_A = 47,182.24$

$SS_C = 46,421.21$

$SS_{AC} = 1,000.05$

$SS_{total} = 93,603.50$

Table 38. Data Summed Over Factors BCE

Level of Factor A

Equivalents of B_2O_3

Level of Factor D, Equivalents of TiO_2	A_1 0 B_2O_3	A_2 0.125 B_2O_3	A_3 0.250 B_2O_3	Total
D_1 0 TiO_2	4,846	5,106	5,430	15,382
D_2 0.100 TiO_2	4,986	5,240	5,553	15,779
D_3 0.200 TiO_2	5,145	5,375	5,589	16,109
Total	14,977	15,721	16,572	47,270

$C = 27,585,838.27$

$C_A = 27,633,020.51$

$C_D = 27,595,653.55$

$C_{AD} = 27,643,558.67$

$SS_A = 47,182.24$

$SS_D = 9,815.28$

$SS_{AD} = 722.88$

$SS_{total} = 57,720.40$

Table 39. Data Summed Over Factors BCD

Level of Factor A

Equivalents of B_2O_3

Level of Factor E, Equivalents of ZrO_2	A_1 0 B_2O_3	A_2 0.125 B_2O_3	A_3 0.250 B_2O_3	Total
E_1 0 ZrO_2	4,866	5,141	5,438	15,445
E_2 0.100 ZrO_2	4,941	5,177	5,495	15,613
E_3 0.200 ZrO_2	5,170	5,403	5,639	16,212
Total	14,977	15,721	16,572	47,270

$C = 27,585,838.27$

$C_A = 27,633,020.51$

$C_E = 27,597,879.18$

$C_{AE} = 27,645,460.67$

$SS_A = 47,182.24$

$SS_E = 12,040.91$

$SS_{AE} = 399.25$

$SS_{total} = 59,622.40$

Table 40. Data Summed Over Factors ADE

Level of Factor B

Equivalents of SiO_2

Level of Factor C
Equivalents of Al_2O_3

	B_1 1.0 SiO_2	B_2 1.5 SiO_2	B_3 2.0 SiO_2	Total
C_1 0 Al_2O_3	4,883	5,075	5,101	15,059
C_2 0.100 Al_2O_3	5,117	5,210	5,267	15,594
C_3 0.200 Al_2O_3	5,462	5,537	5,618	16,617
Total	15,462	15,822	15,986	42,720

$C = 27,585,838.27$

$C_B = 27,591,160.14$

$C_C = 27,632,259.48$

C_{BC} 27,638,036.67

$SS_B = 5,321.87$

$SS_C = 46,421.21$

$SS_{BC} = 455.32$

$SS_{total} = 52,198.40$

Table 41. Data Summed Over Factors ACE

Level of Factor D (Equivalents of TiO_2)	Level of Factor B (Equivalents of SiO_2)			
	B_1 1.0 SiO_2	B_2 1.5 SiO_2	B_3 2.0 SiO_2	Total
D_1 0 TiO_2	4,987	5,167	5,228	15,382
D_2 0.100 TiO_2	5,146	5,260	5,373	15,779
D_3 0.200 TiO_2	5,329	5,395	5,385	16,109
Total	15,462	15,822	15,986	47,270

$C = 27,585,838.27$

$C_B = 27,591,160.14$

$C_D = 27,595,653.55$

$C_{BD} = 27,602,286.44$

$SS_B = 5,321.87$

$SS_D = 9,815.28$

$SS_{BD} = 1,311.02$

$SS_{total} = 16,448.17$

Table 42. Data Summed Over Factors ACD

Level of Factor B

Equivalents of SiO_2

Level of Factor E, Equivalents of ZrO_2	B_1 1.0 SiO_2	B_2 1.5 SiO_2	B_3 2.0 SiO_2	Total
E_1 0 ZrO_2	5,028	5,173	5,244	15,445
E_2 0.100 ZrO_2	5,105	5,203	5,305	15,613
E_3 0.200 ZrO_2	5,329	5,446	5,437	16,212
Total	15,462	15,822	15,986	47,270

$C = 27,585,838.27$

$C_B = 27,591,160.14$

$C_E = 27,597,879.18$

$C_{BE} = 27,603,737.11$

$SS_B = 5,321.87$

$SS_E = 12,040.91$

$SS_{BE} = 536.06$

$SS_{total} = 17,898.84$

Table 43. Data Summed Over Factors ABE

Level of Factor D (Equivalents of TiO_2)	Level of Factor C (Equivalents of Al_2O_3) C_1 0 Al_2O_3	C_2 0.100 Al_2O_3	C_3 0.200 Al_2O_3	Total
D_1 0 TiO_2	4,850	5,131	5,401	15,382
D_2 0.100 TiO_2	5,057	5,160	5,562	15,779
D_3 0.200 TiO_2	5,152	5,303	5,654	16,109
Total	15,059	15,594	16,617	42,720

$C = 28,595,939.27$

$C_C = 27,632,259.48$

$C_D = 27,595,653.55$

$C_{CD} = 27,643,087.11$

$SS_C = 46,421.21$

$SS_D = 9,815.28$

$SS_{CD} = 1,012.35$

$SS_{total} = 57,248.84$

Table 44. Data Summed Over Factors ABD

Level of Factor E (Equivalents of ZrO_2)	Level of Factor C (Equivalents of Al_2O_3)			
	C_1 0 Al_2O_3	C_2 0.100 Al_2O_3	C_3 0.200 Al_2O_3	Total
E_1 0 ZrO_2	4,841	5,170	5,434	15,445
E_2 0.100 ZrO_2	4,958	5,171	5,484	15,613
E_3 0.200 ZrO_2	5,260	5,253	5,699	16,212
Total	15,059	15,594	16,617	47,270

$C = 27,585,838.27$

$C_C = 27,632,259.48$

$C_E = 27,597,879.18$

$C_{CE} = 27,647,556.44$

$SS_C = 46,421.21$

$SS_E = 12,040.91$

$SS_{CE} = 3,256.05$

$SS_{total} = 61,718.17$

Table 45. Data Summed Over Factors ABC

Level of Factor D

Equivalents of TiO_2

	D_1 0 TiO_2	D_2 0.100 TiO_2	D_3 0.200 TiO_2	Total
E_1 0 ZrO_2	4,988	5,195	5,262	16,445
E_2 0.100 ZrO_2	5,061	5,213	5,339	15,613
E_3 0.200 ZrO_2	5,333	5,371	5,508	16,212
Total	15,382	15,779	16,109	47,270

$C = 27,585,838.27$

$C_D = 27,595,653.55$

$C_E = 27,597,879.18$

$C_{DE} = 27,608,602.00$

$SS_D = 9,814.28$

$SS_E = 12,040.91$

$SS_{DE} = 907.54$

$SS_{total} = 22,763.73$

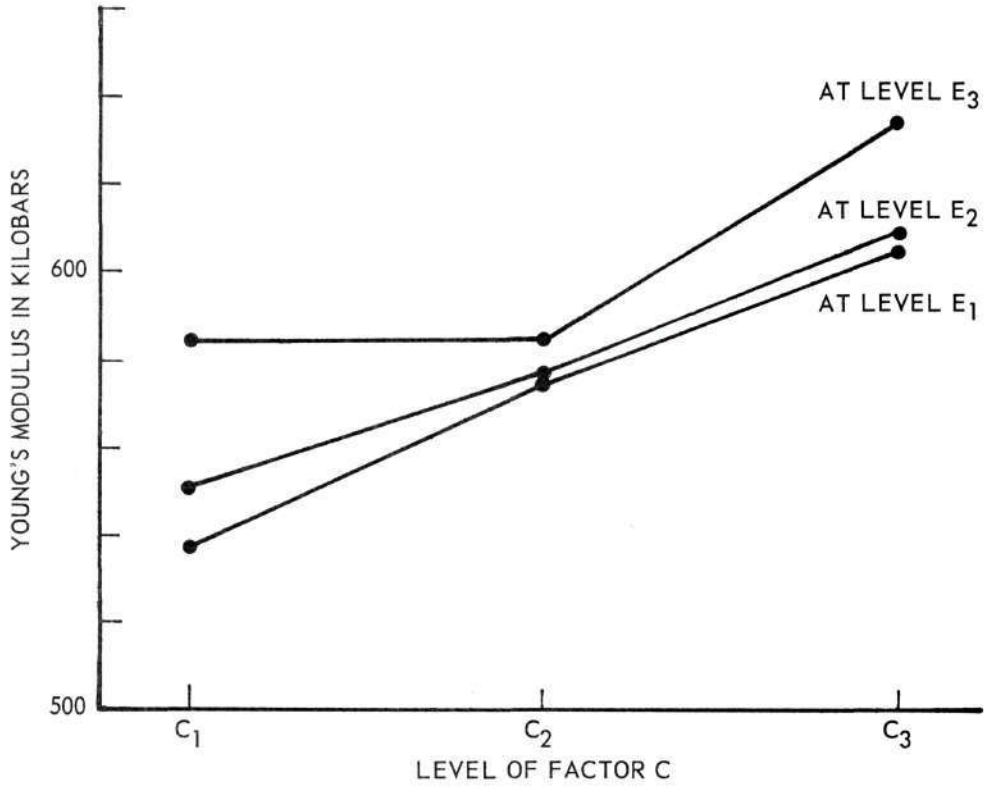

Figure 12. Average Values of Young's Modulus.

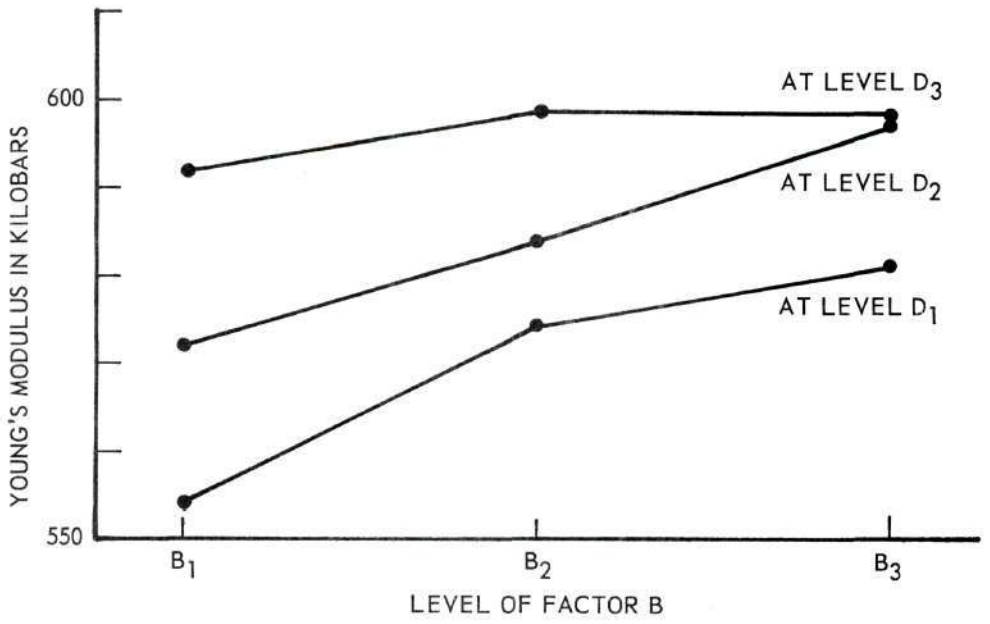

Figure 13. Average Value of Young's Modulus in Kilobars.

Table 46. Duncan's Multiple Range Test For Interactions Design Four

Standard error of mean = $S_{\bar{x}} = \sqrt{\frac{129.62}{9}} = 3.795$

p	Significant Range One Per Cent Level	Least Significant Range One Per Cent Level
2	3.89	15
3	4.06	15

For Alumina-Zirconium Interaction

At Level C_1

Level	E_1	E_2	E_3
Mean	538	551	584

At Level C_2

Level	E_1	E_2	E_3
Mean	574	575	584

At Level C_3

Level	E_1	E_2	E_3
Mean	604	609	633

For TiO_2 - Silica Interaction

At Level D_1

Level	B_1	B_2	B_3
Mean	554	574	581

(Continued)

Table 46. (Continued)

At Level D_2

Level	B_1	B_2	B_3
Mean	572	584	597

At Level D_3

Level	B_1	B_2	B_3
Mean	592	598	599

Table 47. Best Estimate of the Magnitude of the Residual Interactions Plus Experimental Error

Best Estimate = S_o = 11.38 Kilobars

Upper 90 Per Cent Confidence Limit = $\sqrt{\frac{30\, S_o^2}{\chi^2_{0.95;\, 30}}}$ = 14.50 Kilobars

Lower 90 Per Cent Confidence Limit = $\sqrt{\frac{30\, S_o^2}{\chi^2_{0.05;\, 30}}}$ = 9.42 Kilobars

BIBLIOGRAPHY

1. Ajax Magnethermic Corp., Trenton, N. J. "Set-up and Operating Instructions for 6KW Type 'C' Sealed Gap Ajax-Northrup Converter."

2. Akmoran, H., "A Study of the Elasticity of Lead-Bearing Glasses," M. S. Thesis, Alfred University, Box E, 28 (1953).

3. Armistead, W. H., Jr., "Low Expansion Lead Borosilicate Glass of High Chemical Durability," U. S. Patent 2,570,000 (October 2, 1951).

4. ASTM Standards, Book of, "Tentative Method for Average Linear Expansion of Glass," ASTM Designation C33T-54T, Part 3, 922-925, 1955.

5. ASTM Standards, Book of, "Tentative Method for Determination of Young's Modulus at Room Temperature," ASTM Designation E41-55T, Part 3, 1934-37, 1955.

6. ASTM Standards, Book of, "Tentative Method of Test for Fundamental Transverse, Longitudinal, and Torsional Frequencies of Concrete Specimens," ASTM Designation C215-55T, Part 3, 1355-1359, 1955.

7. Ballou, J. W., and Silverman, J. S., "Young's Modulus of Elasticity for Fibers and Films by Sound Velocity Measurements," Textile Research Journal, 14, 282, 1944.

8. Burnett, William H., "Building Units and Method of Producing," U. S. Patent 2,970,060 (January 31, 1961).

9. Bowker, Albert H., and Liberman, Gerald J., Engineering Statistics, Prentice-Hall Inc., Englewood-Cliffs, N. J., 1963.

10. Bryant, E. E., Porcelain Enameling Operations, Enamelist Publishing Co., Cleveland, Ohio, 21-23, 1958.

11. Burroughs Corp., Monrovia, California, Technical Bulletin, ORS-025 (1962).

12. Caruso, Philip A., "New Design Data for Clay Bonded Block," Brick and Clay Record, 135 [4] 69-78, 80, 87 (1959).

13. Chase, George A., "Mechanical Strength of Glasses," Project Report 1-3, Submitted to International Lead-Zinc Research Organization, New York.

14. Clark, J. R., and Turner, W. E. S., Journal of the Society of Glass Technology, 3, 260-266 (1919).

15. Cochran, W. C., and Cox, G. M., Experimental Design, John Wiley and Sons, New York, 1950.

16. Crandall, W. B., and Bryant, C. A., "A Sonic Method of Measuring Young's Modulas of Elasticity at High Temperature," Armed Services Tech. Information Agency, Arlington, Va. (1953).

17. Danzin, A., "Glasses Having a Low Coefficient of Expansion," U. S. Patent 2,469,867 (October 5, 1949); Trans. Brit. Ceram. Soc., 48 420A (1949).

18. Danzin, A., "Lead Glasses of Low Thermal Expansion," Silicates Industry, 18 [8] 321 and [9] 371 (1953).

19. Davies, Owen L., The Design and Analysis of Industrial Experiments, Hafner Publishing Co., New York, 1960.

20. Deyrup, A. J., "Alkali Resistant Glaze," U. S. Patent 2,338,099 (April 1, 1944).

21. Duncan, D. B., "Multiple Range and Multiple F Tests," Statistics Symposium Program, Division of Industrial Engineering Chemistry, 124th Nat'l. Meeting American Chemical Society, Chicago, Ill. (1953).

22. Eico Instrument Company, 84 Withers St., Brooklyn, N. Y., "Manual of Instructions for the Model 460 DC-wide Band Oscilloscope."

23. English, S., and Turner, W. E. S., Journal of the American Ceramic Society 10, 551 (1927), with revisions in J. Am. Ceram. Soc. 12, 760 (1929).

24. Everhart, J. O., "Clay or Shale Makes Lightweight Aggregate," Brick and Clay Record, 134 [5] 58-59, 86 (1959).

25. Fisher, R. A., The Design of Experiments, 6th Edition, Oliver and Boyd, London and Edinburgh, 1951.

26. Fujino, K., Kawai, H., and Horino, T., "Experimental Study of the Visoelastic Properties of Textile Fibers: Dynamic Measurements from Subsonic to Supersonic Frequency," Textile Research Journal, 25, 8 (August 1955).

27. Gilard, P., Dubral, L., Verre Silicates Ind., [5], 122 (1934).

28. Hill, R. D., and Crook, D. N., "Some Causes of Bloating in Expanded Clay and Shale Aggregates," Australian Journal of Applied Science, 11 [3] 374-84 (1960).

29. Hodgman, Charles D., Editor, Handbook of Chemistry and Physics, 40th Edition, Chemical Rubber Publishing Co., Cleveland, Ohio, 3127-8, 1958.

30. Ide, J. M., "Measurement of Young's Modulus," Journal of Geology, 45, 689 (1937).

31. Jones, G. O., "Glass," Methuen's Monographs on Physical Subjects, 1956.

32. Karkhanavala, N. D., "Bibliography on the Expansion of Lead Glass," Glass Industry 33 [8] 403-7 (1952); 33 [9] 458-65 (1952); 33 [10] 526-31, 550 (1952).

33. Kingery, W. D., "Factors Affecting Thermal Stress Resistance of Ceramic Materials," J. Am. Ceram. Soc. 38, 3 (1955).

34. Kingery, W. D., Introduction to Ceramics, John Wiley and Sons, New York and London, 1960.

35. Lead Industries Assoc., New York, "Lead in the Ceramic Industries,"

36. Leiser, Craig F., "Importance of Lead in Glass," Glass Industry 9, 56-59 (1963).

37. Levin, Ernest M., Robins, Carl R., and McMurdie, Howard F., "Phase Diagrams for Ceramists," The American Ceramic Society, Columbus, Ohio, 116, 1964.

38. Levine, I. Sidney, "Organic (Temporary) Binders for Ceramic Systems," Ceramic Age, 75 [1] 39-42; [2] 25-28, 32-36; [3] 29-30 (1960).

39. McNally, Howard L., (to Dow Chem. Co.), "Method of Making Lightweight Aggregate," U. S. 3,059,655 (October 23, 1962).

40. Marguis, John, "Fast-Fire Glazes," Pemco Corp., Baltimore, Maryland.

41. Miller, F. E., and Doeringsfeld, H. A., Mechanics of Materials, International Textbook Co., Scranton, Penn., 1955.

42. Morey, George W., The Properties of Glass, Reinhold Publishing Corp., New York, 1938.

43. Morgan, H. M., "Continuous Non-destructive Testing of Fibers and Yarns," presented at Annual Meeting of the Textile Research Institute (April 1964) Available from H. M. Morgan Co., Inc., 3 Pacific St., Cambridge, Mass. 02139.

44. Osborne, Fred, (to S. P. Kinney Eng., Inc.) "Apparatus for Making Lightweight Aggregates," U. S. Patent 2,978,743 (April 11, 1961).

45. Parmelee, Cullen W., Ceramic Glazes, Industrial Publications Inc., Chicago, Ill., 11-37, 1951.

46. Parsons, M. F., "Basic Rotary Kiln Design for Lightweight Aggregate," Pit and Quarry, 52 [9] 100-104 (1960).

47. Pemco Corp., Baltimore, Maryland, "Suggested Glaze Batches for Fast Fire Glazes," Tech. Bull. 5015.

48. Phillips, C. J., "Calculation of Young's Modulus of Elasticity from Composition of Simple and Complex Silicate Glasses," Glass Technology, 5 [6] (December, 1964).

49. Robinson, G. C., "Clay Bonded Block," Brick and Clay Record, 134 [2] 38-40, 60-61 (1959).

50. Singer, F., "Low-Temperature Glazes," Trans. Brit. Ceram. Soc., 53, 398 (1954).

51. Sinnott, Maurice J., The Solid State for Engineers, John Wiley and Sons, New York, 295-7, 1958.

52. Smith, T. A., "Organic Binders and Other Additives for Glazes and Engobes," Transactions of the British Ceramic Society 61 [9] 523-49 (1962).

53. Spinner, S., "Elastic Modulii of Glasses by a Dynamic Method," J. Am. Ceram. Soc. 37 [5] 229-34 (1954).

54. Stanworth, J., Physical Properties of Glass, Oxford Press, Toronto, 1950.

55. Straubel, R., Ann. Physik Chem., 68,369-413 (1899).

56. Strobel, G., "A Simple Method for the Determination of the Expansion Coefficients of Enamels," Sprechsaal fur Keramik, Glas, Email (1961).

57. Timoshenko, S., Theory of Elasticity, McGraw-Hill Book Co., New York, 1934.

58. Tinker, Dean, "Commercial Production of Clay Block in Plant," Brick and Clay Record, 135 [4] 69 - 78, 80, 87 (1959).

59. Thomas M., "The Purpose and Measurement of the Thermal Expansion of Glass," J. Soc. Glass Tech., 12 [3] 98-103 (1928).

60. Wilson, H. S., "Development of the Canadian Lightweight Aggregate Industry," Journal of the Canadian Ceramic Society 30, 7-14 (1961).

61. Winkelmann, A., and Schott, C., Ann. Physik., 51, 735 (1894). Hovestadt, H., "Jena Glass," trans. by Everett, J. D. and Everett, A., Macmillan, New York (1902).